The global water resources and use model WaterGAP v2.2e: description and evaluation of modifications and new features - Supplementary material

Hannes Müller Schmied[1,2], Tim Trautmann[1], Sebastian Ackermann[1], Denise Cáceres[1], Martina Flörke[3], Helena Gerdener[4], Ellen Kynast[5], Thedini Asali Peiris[1], Leonie Schiebener[1], Maike Schumacher[6], and Petra Döll[1,2]

[1]Institute of Physical Geography, Goethe University Frankfurt, Frankfurt am Main, Germany
[2]Senckenberg Leibniz Biodiversity and Climate Research Centre (SBiK-F), Frankfurt am Main, Germany
[3]Engineering Hydrology and Water Resources Management, Ruhr-University of Bochum, Bochum, Germany
[4]Institute of Geodesy and Geoinformation, University of Bonn, Bonn, Germany
[5]Center for Environmental Systems Research, University of Kassel, Kassel, Germany
[6]Geodesy Group, Department of Planning, Aalborg University, Denmark

Correspondence: hannes.mueller.schmied@em.uni-frankfurt.de

S1 Additional tables

This section consists of additional Tables, which might help to understand specific contents of the main text.

S2 Additional figures

This section consists of additional figures, which might help to understand specific contents of the main text. Please note that only some of the figures are referenced in the main paper, but we are providing also several additional figures to provide insight into specific aspects. The following figures are shown:

- S1-S2: comparison of simulated and observed water storage variations in reservoirs
- S3: effect of the accidental used lower amount of calibration years
- S4-S7: calibration parameters for the other 4 model variants
- S8-S11: comparison of potential water withdrawal uses with AQUASTAT for the other 4 model variants
- S12-S13: efficiency metrics for calibration and validation data (streamflow)
- S14-S23: cumulative distribution of performance metrics for calibration and validation data (streamflow)
- S24-S37: maps with NSE performance indicators and the model variants (streamflow)
- S38-S51: maps with KGE and its components and the model variants (streamflow)
- S52-S55: comparison of TWSA for the other 4 model variants
- S56-S58: seasonality of streamflow and TWSA for 12 large river basins and different combinations of model variants

Table S1. List of reservoirs used for comparison between observed and simulated monthly reservoir storage. Data source (column S): a: California Department of Water Resources, b: Bureau of Reclamation, c: Texas Water Development Board

Reservoir name	S	Lon	Lat	USA state	Main use	Area (km^2)	Volume (km^3)
Lake Berryessa	a	-122.22	38.59	California	irrigation	66.6	1.96
Cascade reservoir	b	-116.1	44.63	Idaho	irrigation	103.7	0.81
New Don Pedro reservoir	a	-120.42	37.7	California	irrigation	41.6	2.50
Hungry Horse reservoir	b	-114.01	48.34	Montana	irrigation	75.3	3.68
Amistad lake	c	-101.05	29.45	Texas	irrigation	131.5	6.33
Livingston reservoir	c	-95.02	30.63	Texas	flood	219.6	2.52
Mohave lake	a	-114.66	35.47	California	electricity	113.4	2.24
New Melones reservoir	a	-120.52	37.95	California	irrigation	43.2	2.98
Oroville lake	a	-121.49	39.62	California	flood	68.5	4.37
Palisades reservoir	b	-111.12	43.24	Idaho	irrigation	64.5	1.48
Pine Flat lake	a	-119.32	36.83	California	flood	15.4	1.23
Powell lake	a	-110.73	37.37	California	electricity	647.8	25.07
Richland-Chambers reservoir	c	-96.1	31.97	Texas	recreation	156.5	2.15
Sam Rayburn reservoir	c	-94.11	31.07	Texas	supply	380.1	7.82
San Luis reservoir	a	-121.13	37.05	California	irrigation	50	2.42
Toledo Bend reservoir	c	-93.57	31.18	Texas	electricity	599.6	6.29

Table S2. Global-scale (excluding Antarctica and Greenland) water balance components for different time spans as simulated with WaterGAP 2.2d with gswp3-w5e5. All units in $km^3 yr^{-1}$. Long-term average volume balance error is calculated as the difference of component 1 and the sum of components 2,3 and 8.

No.	Component	1961-1990	1971-2000	1981-2010	1991-2019	2001-2019
1	Precipitation	110637	111279	111351	111575	111657
2	Actual evapotranspiration[1]	70577	70983	71042	71184	71245
3	Streamflow into oceans and inland sinks	40045	40305	40366	40495	40537
4	Inflow into inland sinks[2]	773	791	791	837	842
5	Actual consumptive water use[3]	917	1063	1212	1324	1388
6	Actual net abstraction from surface water	1024	1169	1315	1420	1470
7	Actual net abstraction from groundwater	-107	-106	-103	-96	-83
8	Change of total water storage	14	-9	-56	-104	-125
9	Long-term average volume balance error	0.37	0.25	0.13	0.03	0.01

[1] including actual consumptive water use

[2] streamflow that flows into inland sinks; the simulated streamflow of inland sinks is added to actual evapotranspiration

[3] sum of rows 6 and 7

Table S3. Global-scale (excluding Antarctica and Greenland) water balance components for different time spans as simulated with WaterGAP 2.2e with 20crv3-era5. All units in $km^3 yr^{-1}$. Long-term average volume balance error is calculated as the difference of component 1 and the sum of components 2,3 and 8.

No.	Component	1961-1990	1971-2000	1981-2010	1991-2019	2001-2021
1	Precipitation	120548	121272	120244	118878	117604
2	Actual evapotranspiration[1]	79976	80514	79900	78886	77988
3	Streamflow into oceans	40540	40766	40441	40127	39759
4	Inflow into inland sinks[2]	1106	1086	1031	992	955
5	Actual consumptive water use[3]	852	984	1123	1230	1295
6	Actual net abstraction from surface water	962	1094	1241	1347	1407
7	Actual net abstraction from groundwater	-110	-110	-118	-118	-112
8	Change of total water storage	32	-8	-97	-135	-143
9	Long-term average volume balance error	-0.34	-0.21	-0.08	0.04	0.02

[1] including actual consumptive water use

[2] streamflow that flows into inland sinks; the simulated streamflow of inland sinks is added to actual evapotranspiration

[3] sum of rows 6 and 7

Table S4. Global-scale (excluding Antarctica and Greenland) water balance components for different time spans as simulated with WaterGAP 2.2e with 20crv3-w5e5. All units in km^3yr^{-1}. Long-term average volume balance error is calculated as the difference of component 1 and the sum of components 2,3 and 8.

No.	Component	1961-1990	1971-2000	1981-2010	1991-2019	2001-2019
1	Precipitation	111227	111284	111350	111574	111655
2	Actual evapotranspiration[1]	71456	71834	71923	72106	72170
3	Streamflow into oceans	39769	39461	39478	39557	39591
4	Inflow into inland sinks[2]	881	831	789	835	840
5	Actual consumptive water use[3]	899	1039	1183	1293	1354
6	Actual net abstraction from surface water	1022	1167	1320	1428	1479
7	Actual net abstraction from groundwater	-123	-128	-136	-135	-125
8	Change of total water storage	2	-11	-51	-90	-106
9	Long-term average volume balance error	-0.45	-0.34	-0.21	-0.08	-0.07

[1] including actual consumptive water use

[2] streamflow that flows into inland sinks; the simulated streamflow of inland sinks is added to actual evapotranspiration

[3] sum of rows 6 and 7

Table S5. Global-scale (excluding Antarctica and Greenland) water balance components for different time spans as simulated with WaterGAP 2.2e with gswp3-era5. All units in km^3yr^{-1}. Long-term average volume balance error is calculated as the difference of component 1 and the sum of components 2,3 and 8.

No.	Component	1961-1990	1971-2000	1981-2010	1991-2019	2001-2022
1	Precipitation	120374	121389	120244	118878	117569
2	Actual evapotranspiration[1]	80079	80546	79851	78843	77895
3	Streamflow into oceans	40255	40853	40493	40169	39844
4	Inflow into inland sinks[2]	980	1044	1038	1000	957
5	Actual consumptive water use[3]	854	987	1129	1237	1306
6	Actual net abstraction from surface water	965	1099	1249	1359	1422
7	Actual net abstraction from groundwater	-111	-112	-121	-121	-116
8	Change of total water storage	40	-10	-100	-134	-169
9	Long-term average volume balance error	-0.54	-0.40	-0.24	-0.11	-0.10

[1] including actual consumptive water use

[2] streamflow that flows into inland sinks; the simulated streamflow of inland sinks is added to actual evapotranspiration

[3] sum of rows 6 and 7

Table S6. Globally aggregated (excluding Antarctica and Greenland) water storage component changes during different time periods as simulated by WaterGAP 2.2d with gswp3-w5e5. All units in km^3yr^{-1}.

No.	Component	1961-1990	1971-2000	1981-2010	1991-2019	2001-2019
1	Canopy	0	0	0.1	0	0
2	Snow	11.4	-9.2	-2.5	-13.7	-0.8
3	Soil	4.9	7.5	9.4	-0.2	-8.7
4	Groundwater	-66.7	-73	-99.6	-118.1	-142.7
5	Local lakes	0.1	1	0.8	0.3	-1.3
6	Local wetlands	0.8	-0.6	4.6	4.2	9.1
7	Global lakes	-2	-1	-0.4	4.8	8.8
8	Global wetlands	-3.7	4.9	0.8	0.2	-7
9	Reservoirs and regulated lakes	72.2	50.8	30.8	11	5.1
10	River	0.4	5.4	-8.2	3.4	3.5
11	Total water storage	17.4	-14.2	-64.2	-108.2	-134.1

Table S7. Globally aggregated (excluding Antarctica and Greenland) water storage component changes during different time periods as simulated by WaterGAP 2.2e with 20crv3-era5. All units in km^3yr^{-1}.

No.	Component	1961-1990	1971-2000	1981-2010	1991-2019	2001-2021
1	Canopy	0	0	0	0	0
2	Snow	16.4	3.1	-4.4	-21.5	-16.7
3	Soil	6.7	4.7	-1.6	-8.8	-3.3
4	Groundwater	-62.6	-70.7	-107.2	-126.7	-149.9
5	Local lakes	-0.1	1.7	2.3	1.8	1.3
6	Local wetlands	-1.0	4.9	1.5	8.5	3.7
7	Global lakes	-3.7	-1.6	-4.6	-0.2	-2.4
8	Global wetlands	-0.9	4.1	-6.0	-7.0	-11.6
9	Reservoirs and regulated lakes	71.7	49.9	27.9	16.5	24.3
10	River	1.9	-7.8	-12.5	-0.2	-7.3
11	Total water storage	28.3	-11.6	-104.5	-137.6	-162.0

Table S8. Globally aggregated (excluding Antarctica and Greenland) water storage component changes during different time periods as simulated by WaterGAP 2.2e with 20crv3-w5e5. All units in km^3yr^{-1}.

No.	Component	1961-1990	1971-2000	1981-2010	1991-2019	2001-2019
1	Canopy	0	0	0.1	0	0
2	Snow	11.1	-4.1	-0.9	-13.3	-0.8
3	Soil	4.2	7.7	9.5	0.2	-7.9
4	Groundwater	-71.2	-71.3	-96.3	-117.9	-145.2
5	Local lakes	-1.1	0.9	0.8	0.2	-1.3
6	Local wetlands	1.0	3.8	4.4	4.4	9.3
7	Global lakes	-5.7	-3.2	-2.9	4.0	9.8
8	Global wetlands	-2.5	6.3	0.6	0.3	-7.1
9	Reservoirs and regulated lakes	67.5	53.0	34.3	25.5	24.3
10	River	-3.2	-10.4	-8.3	3.8	4.2
11	Total water storage	0.1	-17.5	-58.6	-92.7	-114.8

Table S9. Globally aggregated (excluding Antarctica and Greenland) water storage component changes during different time periods as simulated by WaterGAP 2.2e with gswp3-era5. All units in km^3yr^{-1}.

No.	Component	1961-1990	1971-2000	1981-2010	1991-2019	2001-2022
1	Canopy	0	0	0	0	0
2	Snow	20.3	-1.1	-6.3	-20.2	-14.1
3	Soil	6.2	3.6	-1.7	-8.8	-12.5
4	Groundwater	-62.4	-73.8	-107.0	-125.8	-150.3
5	Local lakes	1.3	2.0	2.4	1.8	-1.0
6	Local wetlands	-1.0	1.4	1.7	8.5	3.6
7	Global lakes	-0.1	-0.2	-4.3	-0.4	-4.4
8	Global wetlands	-2.3	2.0	-5.9	-7.0	-8.6
9	Reservoirs and regulated lakes	73.8	47.0	25.7	15.3	19.4
10	River	2.1	3.4	-12.4	-0.3	-16.6
11	Total water storage	38.0	-15.7	-107.7	-136.8	-184.7

Table S10. Globally aggregated (excluding Antarctica and Greenland) sectoral potential withdrawal water use WU and consumptive water use CU ($km^3 yr^{-1}$) as well as use fractions from groundwater (%) as simulated by GWSWUSE of WaterGAP 2.2d with gswp3-w5e5 for the time period 1991-2019. These values represent demand for water that cannot be completely satisfied in WGHM due to lack of surface water resources (row 5 in Table S2)

Water use sector	WU	Percent of WU from groundwater	CU	Percent of CU from groundwater
Irrigation	2541	25	1179	37
Thermal power plants	601	0	16	0
Domestic	352	36	57	37
Manufacturing	278	27	56	26
Livestock	29	0	29	0
Total	3801	22	1336	36

Table S11. Globally aggregated (excluding Antarctica and Greenland) sectoral potential withdrawal water use WU and consumptive water use CU ($km^3 yr^{-1}$) as well as use fractions from groundwater (%) as simulated by GWSWUSE of WaterGAP 2.2e with 20crv3-era5 for the time period 1991-2019. These values represent demand for water that cannot be completely satisfied in WGHM due to lack of surface water resources (row 5 in Table S3)

Water use sector	WU	Percent of WU from groundwater	CU	Percent of CU from groundwater
Irrigation	2378	25	1106	37
Thermal power plants	592	0	18	0
Domestic	352	35	57	36
Manufacturing	298	27	60	25
Livestock	29	0	29	0
Total	3650	22	1269	35

Table S12. Globally aggregated (excluding Antarctica and Greenland) sectoral potential withdrawal water use WU and consumptive water use CU ($km^3 yr^{-1}$) as well as use fractions from groundwater (%) as simulated by GWSWUSE of WaterGAP 2.2e with 20crv3-w5e5 for the time period 1991-2019. These values represent demand for water that cannot be completely satisfied in WGHM due to lack of surface water resources (row 5 in Table S4)

Water use sector	WU	Percent of WU from groundwater	CU	Percent of CU from groundwater
Irrigation	2541	25	1179	37
Thermal power plants	592	0	18	0
Domestic	352	35	57	36
Manufacturing	298	27	60	25
Livestock	29	0	29	0
Total	3813	22	1342	35

Table S13. Globally aggregated (excluding Antarctica and Greenland) sectoral potential withdrawal water use WU and consumptive water use CU ($km^3 yr^{-1}$) as well as use fractions from groundwater (%) as simulated by GWSWUSE of WaterGAP 2.2e with gswp3-era5 for the time period 1991-2019. These values represent demand for water that cannot be completely satisfied in WGHM due to lack of surface water resources (row 5 in Table S5)

Water use sector	WU	Percent of WU from groundwater	CU	Percent of CU from groundwater
Irrigation	2376	25	1105	37
Thermal power plants	592	0	18	0
Domestic	352	35	57	36
Manufacturing	298	27	60	25
Livestock	29	0	29	0
Total	3648	22	1268	35

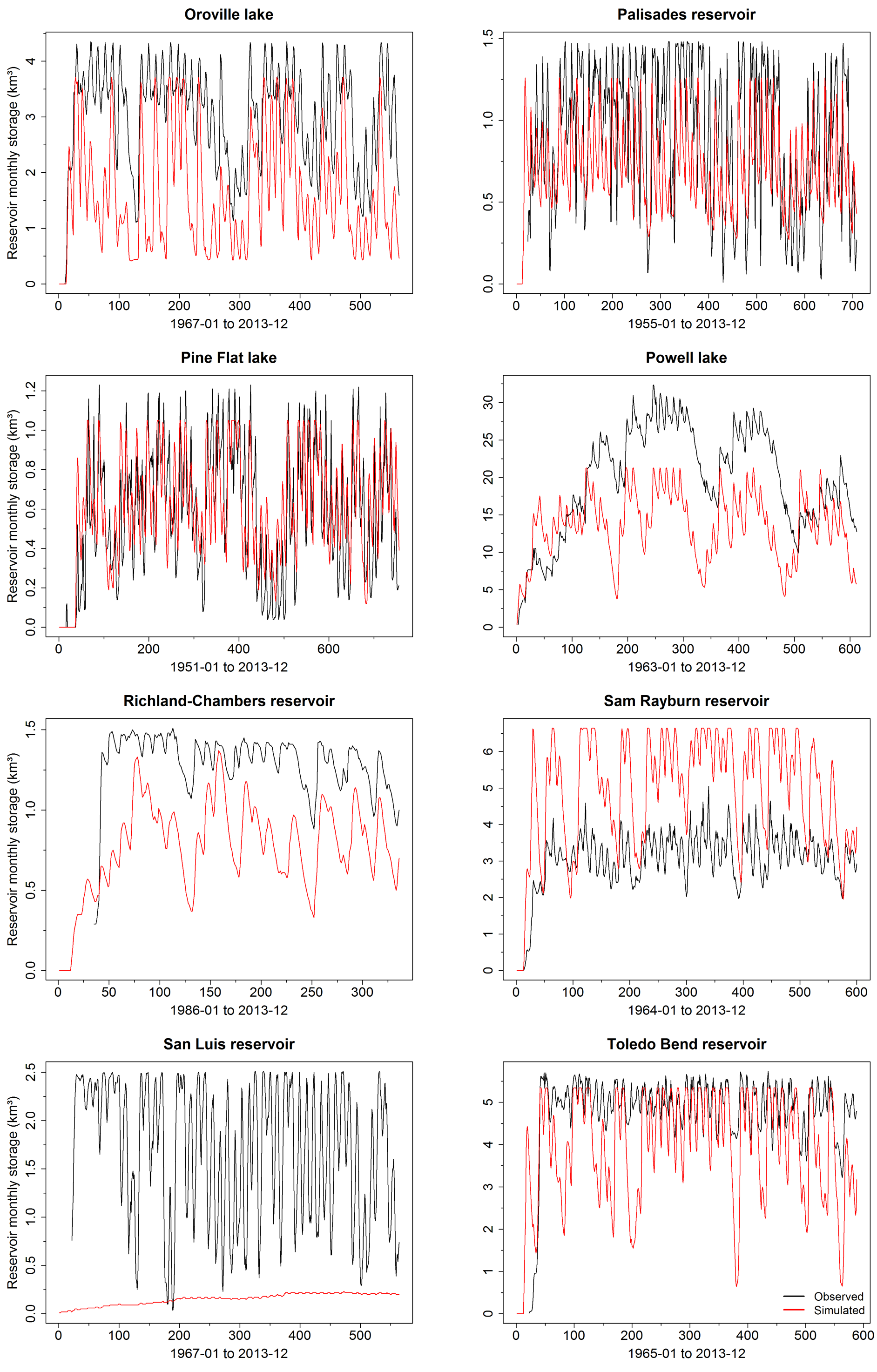

Figure S1. Comparison of simulated (with WaterGAP 2.2c) and observed water storage variations in reservoirs (Part 1)

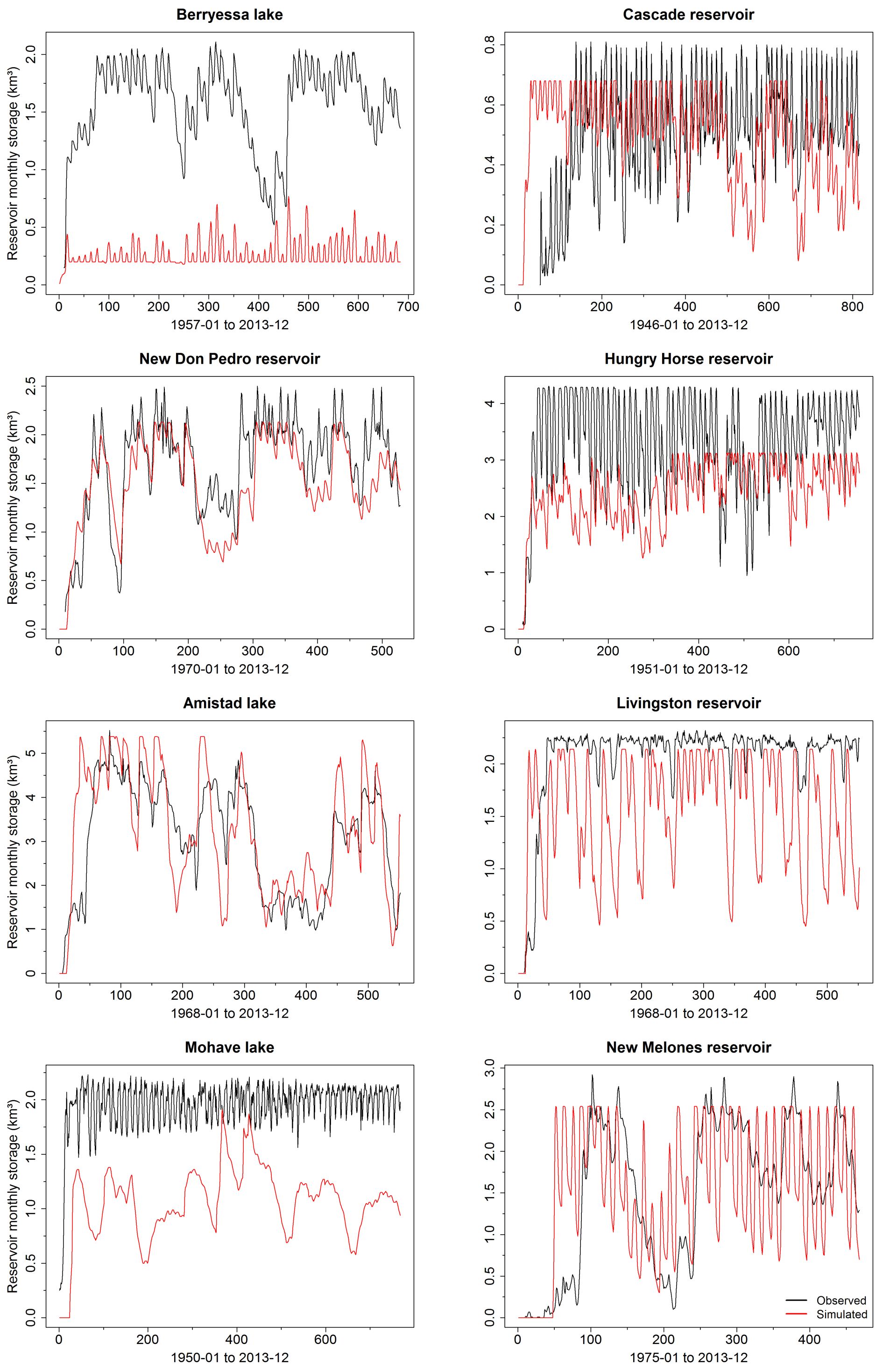

Figure S2. Comparison of simulated (with WaterGAP 2.2c) and observed water storage variations in reservoirs (Part 2)

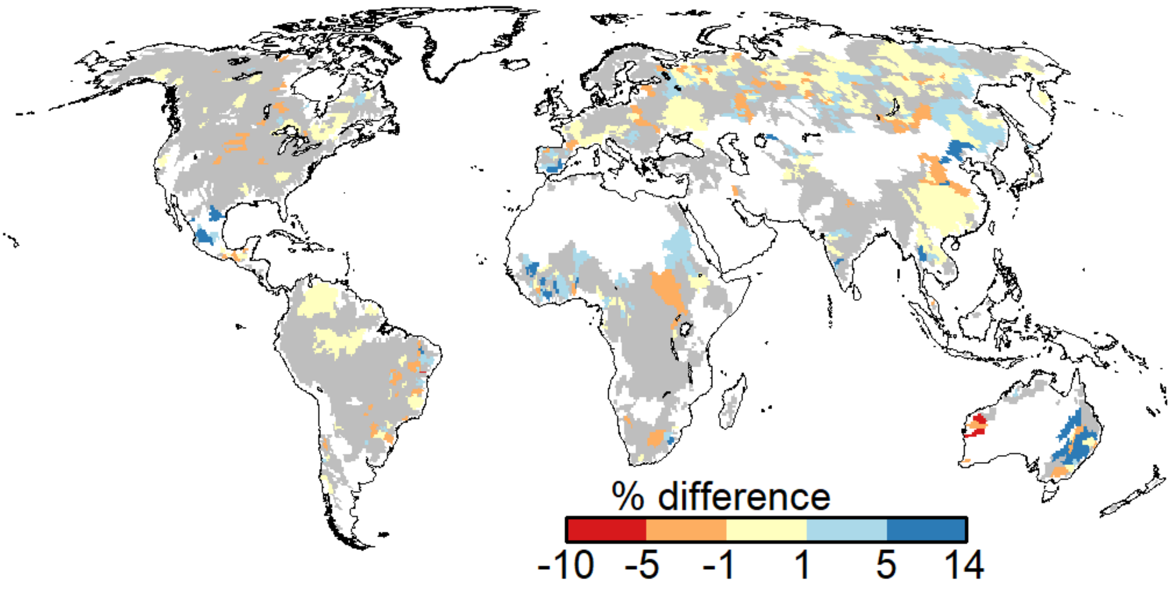

Figure S3. Per cent difference of mean monthly observed streamflow that resulted from neglecting one or two years for calibration as compared to full 30 years of calibration. Bluish colours mean that by using 30 years instead of less years, more streamflow would be taken into account for calibration (and vice versa for reddish colours). The issue is not affecting the grey areas.

.

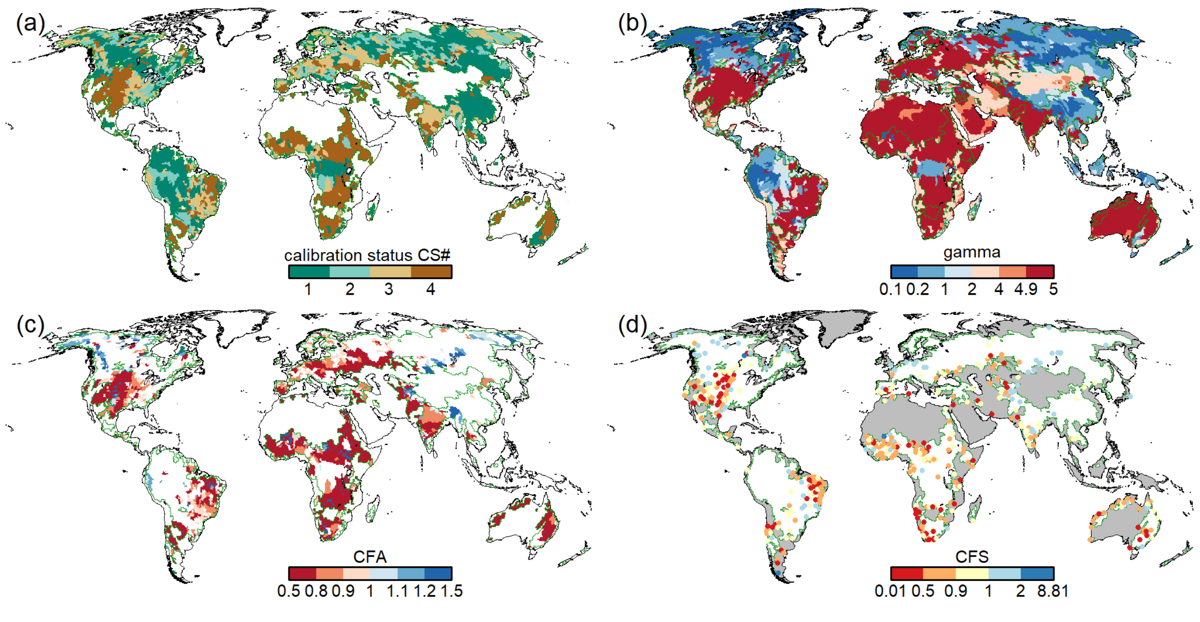

Figure S4. Results of the calibration of WaterGAP 2.2d to the gswp3-w5e5 climate forcing with (a) the calibration status of each calibration basin, (b) calibration parameter γ, (c) areal correction factor CFA and (d) station correction factor CFS. Grey areas in (d) indicate regions with regionalized calibration parameter γ and for (a)-(d) dark green outlines indicate the boundaries of the calibration basins. For details to the calibration procedure the reader is referred to Müller Schmied et al. (2021)

.

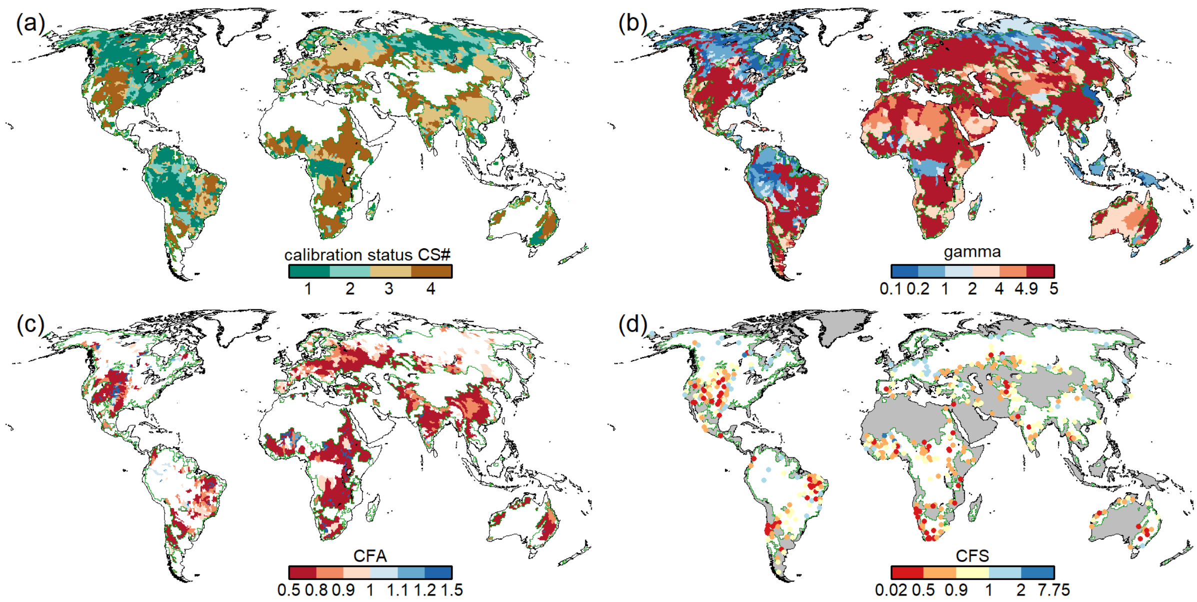

Figure S5. Results of the calibration of WaterGAP 2.2e to the gswp3-era5 climate forcing with (a) the calibration status of each calibration basin, (b) calibration parameter γ, (c) areal correction factor CFA and (d) station correction factor CFS. Grey areas in (d) indicate regions with regionalized calibration parameter γ and for (a)-(d) dark green outlines indicate the boundaries of the calibration basins. For details to the calibration procedure the reader is referred to Müller Schmied et al. (2021)

.

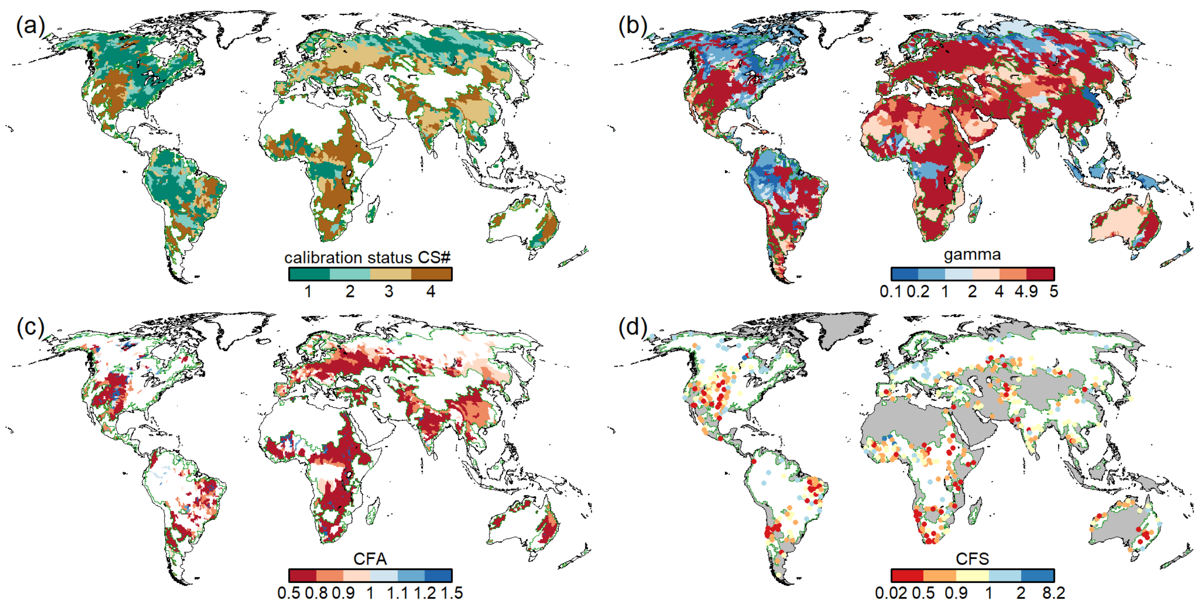

Figure S6. Results of the calibration of WaterGAP 2.2e to the 20crv3-era5 climate forcing with (a) the calibration status of each calibration basin, (b) calibration parameter γ, (c) areal correction factor CFA and (d) station correction factor CFS. Grey areas in (d) indicate regions with regionalized calibration parameter γ and for (a)-(d) dark green outlines indicate the boundaries of the calibration basins. For details to the calibration procedure the reader is referred to Müller Schmied et al. (2021)

.

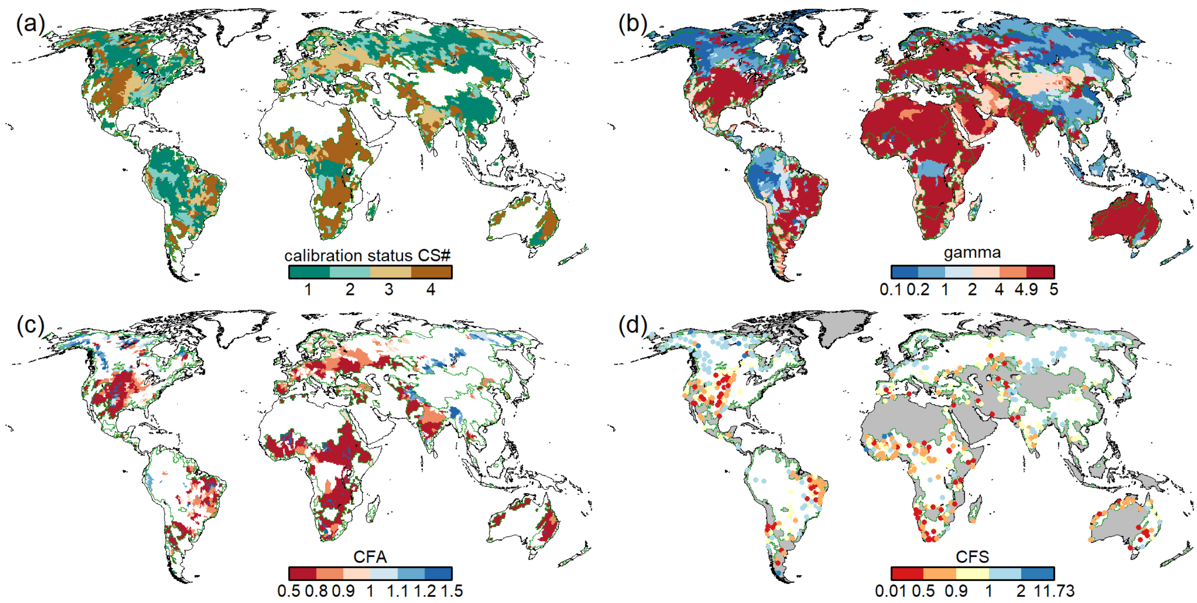

Figure S7. Results of the calibration of WaterGAP 2.2e to the 20crv3-w5e5 climate forcing with (a) the calibration status of each calibration basin, (b) calibration parameter γ, (c) areal correction factor CFA and (d) station correction factor CFS. Grey areas in (d) indicate regions with regionalized calibration parameter γ and for (a)-(d) dark green outlines indicate the boundaries of the calibration basins. For details to the calibration procedure the reader is referred to Müller Schmied et al. (2021)

.

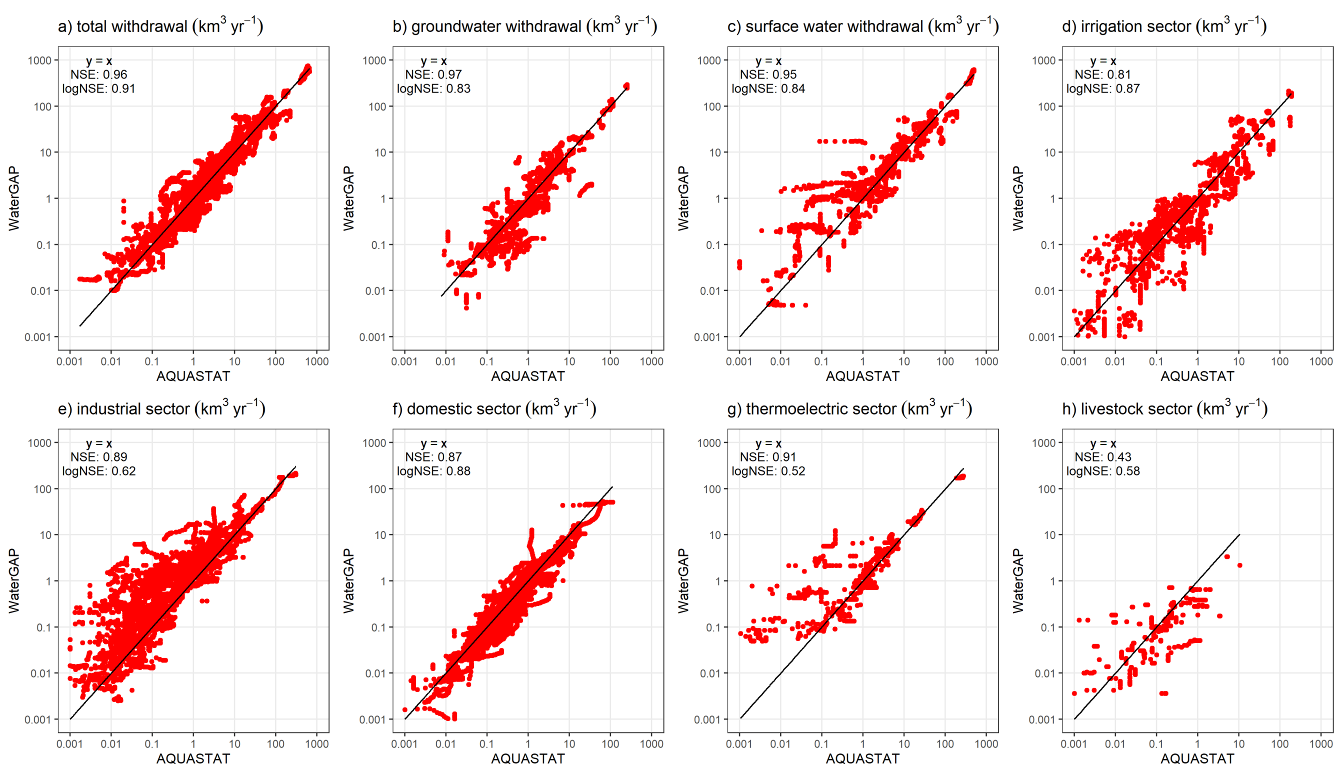

Figure S8. Comparison of potential withdrawal water uses from WaterGAP 2.2d and gswp3-w5e5 with AQUASTAT (FAO, 2023). Each data point represents one yearly value (if present in the database) per country for the time span 1964-2019.

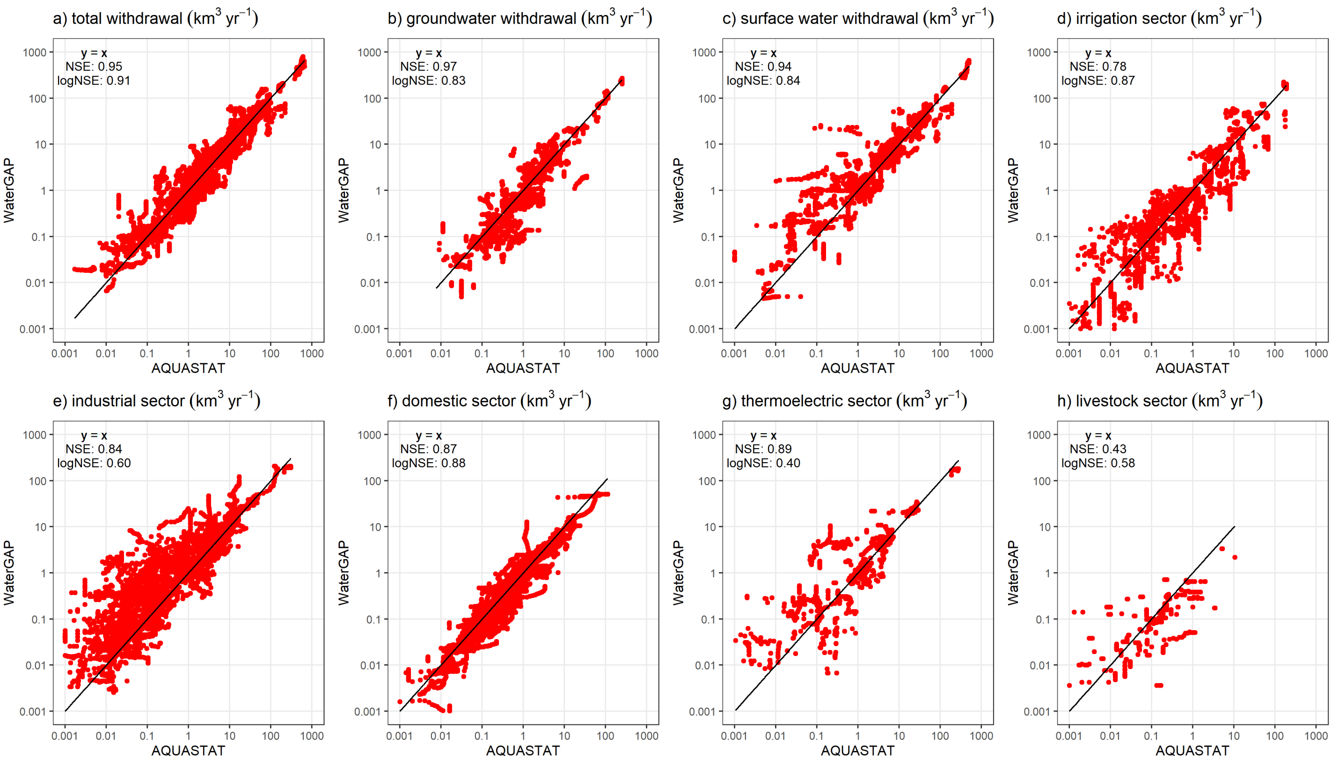

Figure S9. Comparison of potential withdrawal water uses from WaterGAP 2.2e and 20crv3-era5 with AQUASTAT (FAO, 2023). Each data point represents one yearly value (if present in the database) per country for the time span 1964-2019.

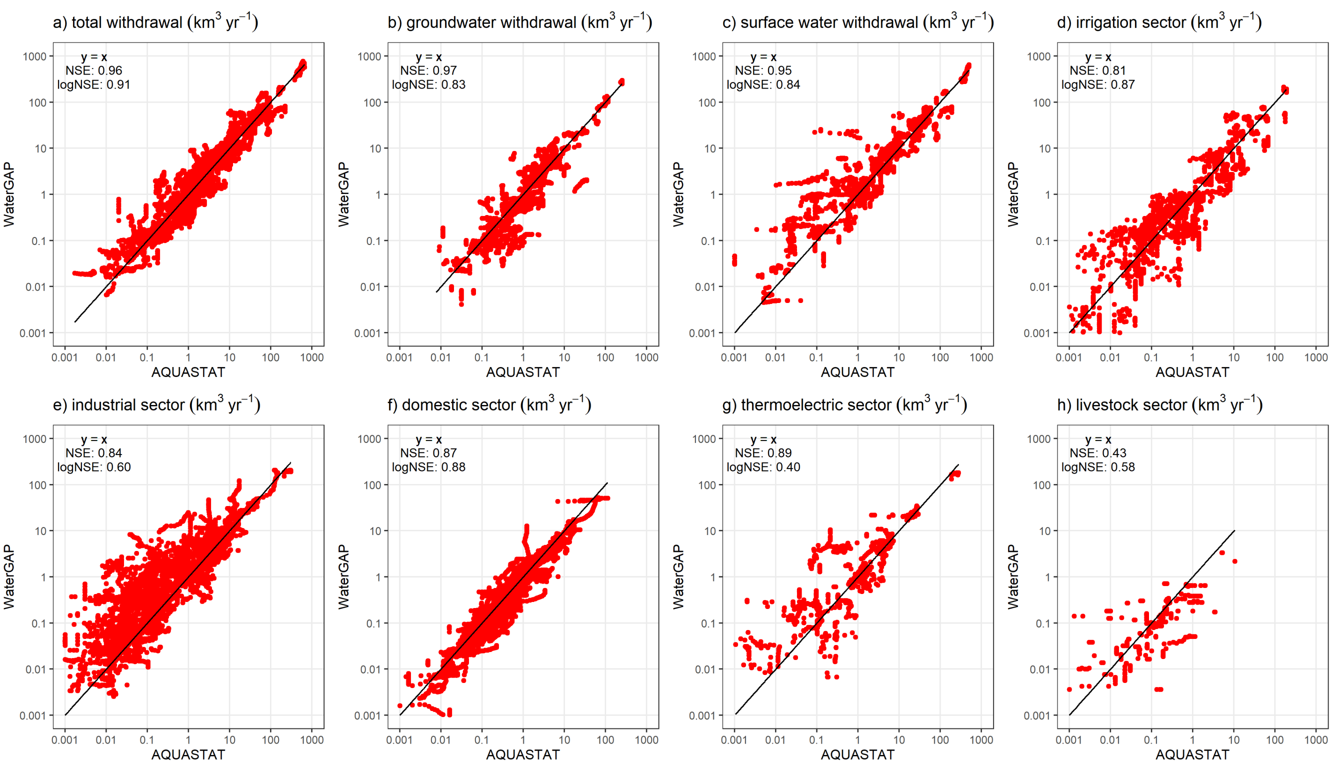

Figure S10. Comparison of potential withdrawal water uses from WaterGAP 2.2e and 20crv3-w5e5 with AQUASTAT (FAO, 2023). Each data point represents one yearly value (if present in the database) per country for the time span 1964-2019.

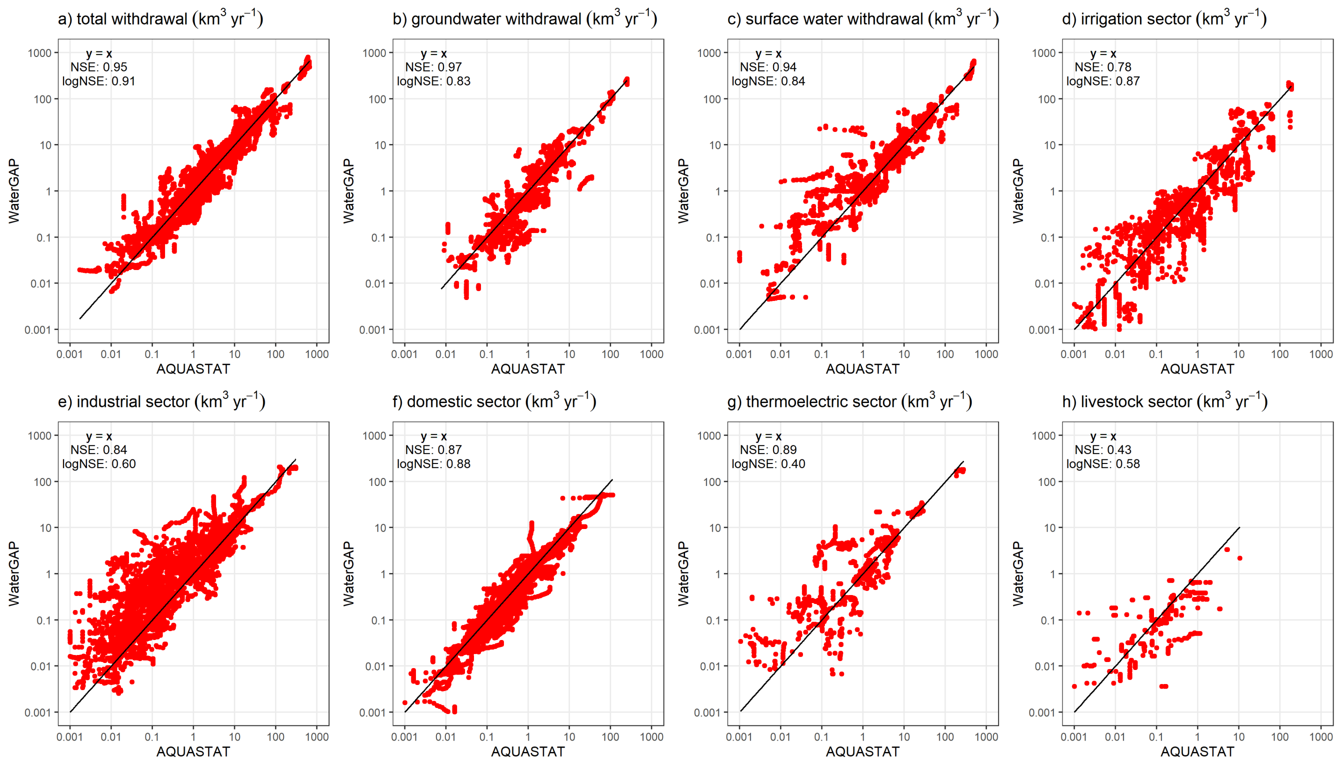

Figure S11. Comparison of potential withdrawal water uses from WaterGAP 2.2e and gswp3-era5 with AQUASTAT (FAO, 2023). Each data point represents one yearly value (if present in the database) per country for the time span 1964-2019.

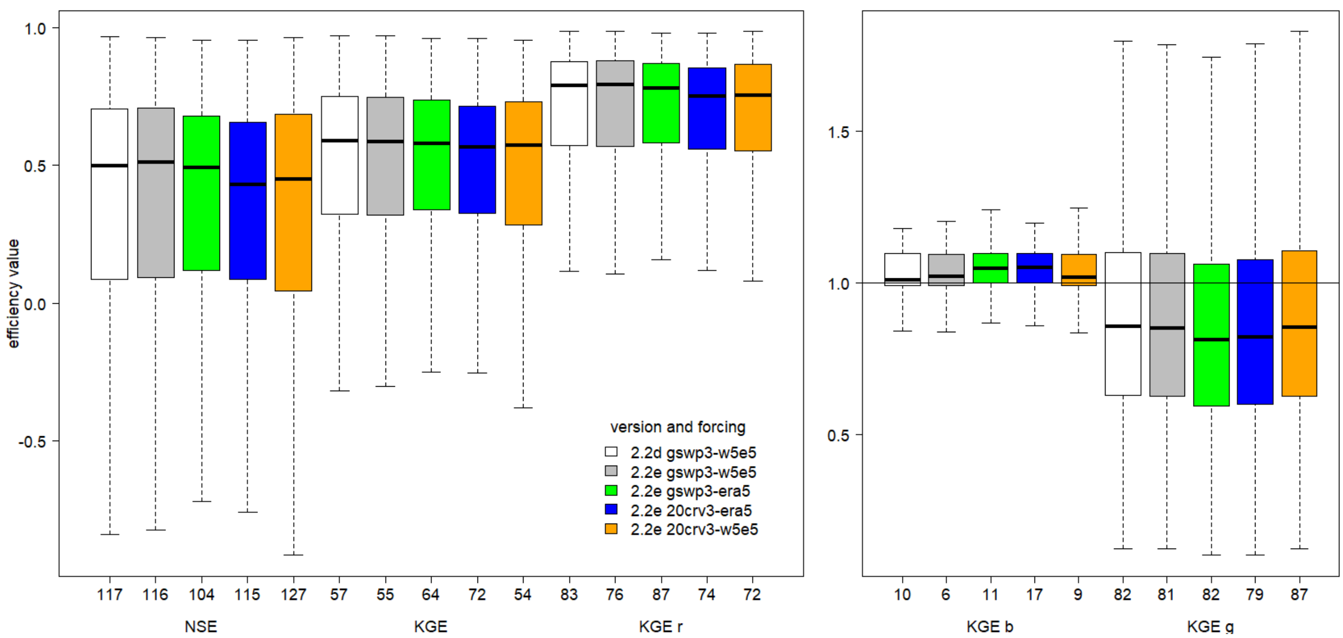

Figure S12. Efficiency metrics for monthly streamflow of the WaterGAP variants at the 1509 observation stations (calibration data) with NSE, KGE and its components. Outliers (outside 1.5× inter-quartile range) are excluded but the number of stations that are defined as outliers are indicated after the metric.

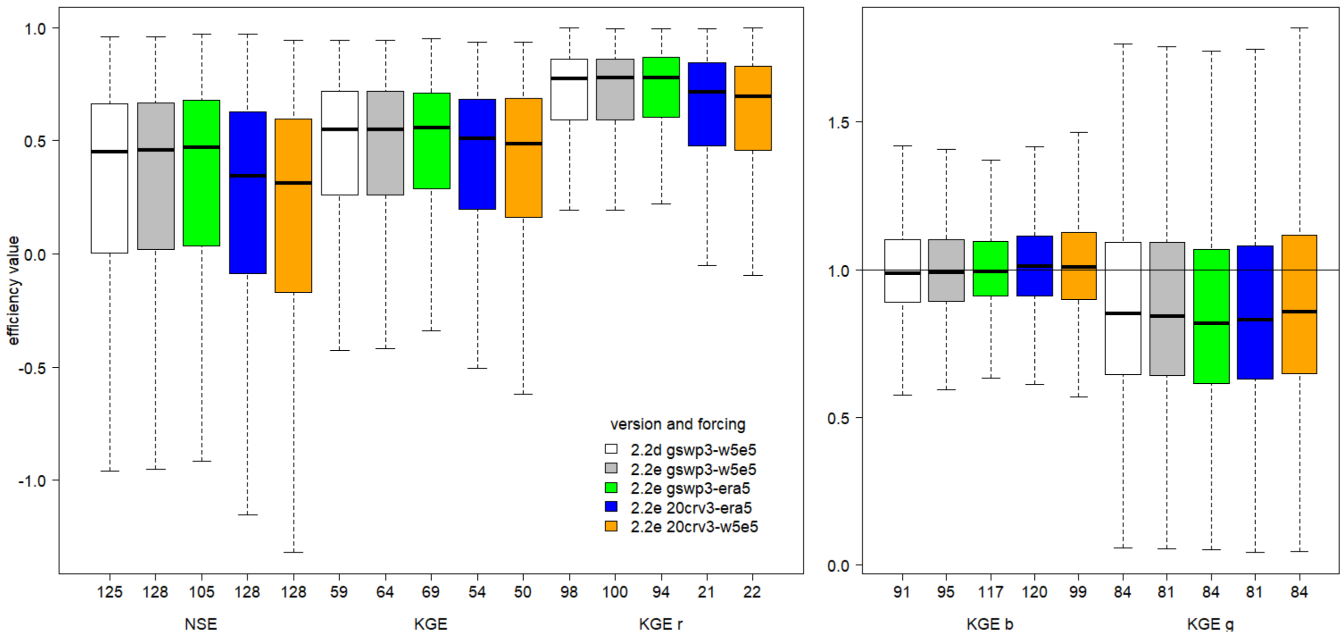

Figure S13. Efficiency metrics for monthly streamflow of the WaterGAP variants at the 1509 observation stations (validation data) with NSE, KGE and its components. Outliers (outside 1.5× inter-quartile range) are excluded but the number of stations that are defined as outliers are indicated after the metric.

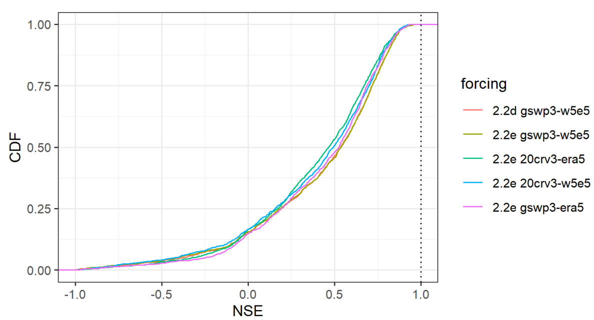

Figure S14. Cumulative distribution of the NSE efficiency metric for calibration streamflow values at the 1509 gauging stations for all model variants.

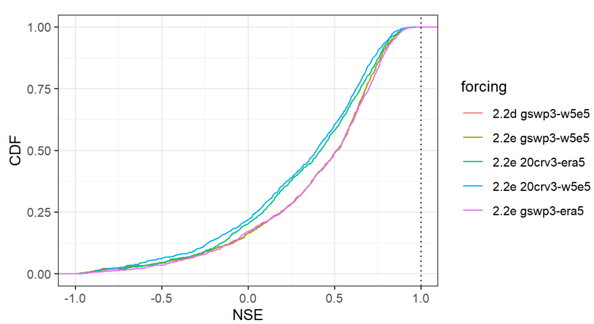

Figure S15. Cumulative distribution of the NSE efficiency metric for validation streamflow values at the 1509 gauging stations for all model variants.

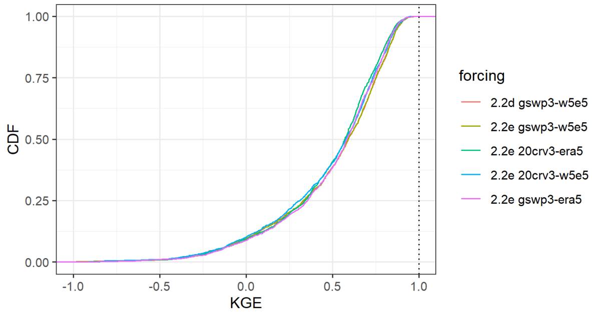

Figure S16. Cumulative distribution of the KGE efficiency metric for calibration streamflow values at the 1509 gauging stations for all model variants.

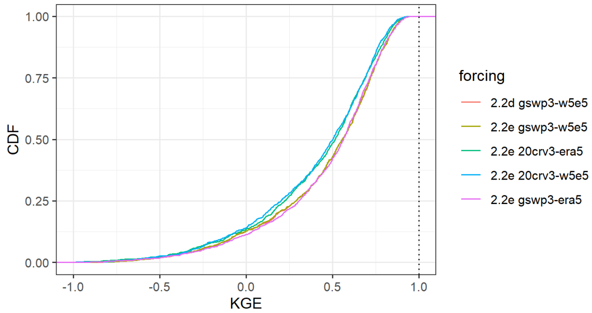

Figure S17. Cumulative distribution of the KGE efficiency metric for validation streamflow values at the 1509 gauging stations for all model variants.

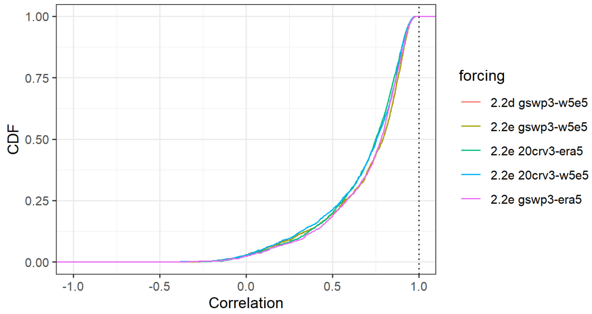

Figure S18. Cumulative distribution of the KGE efficiency metric (correlation parameter) for calibration streamflow values at the 1509 gauging stations for all model variants.

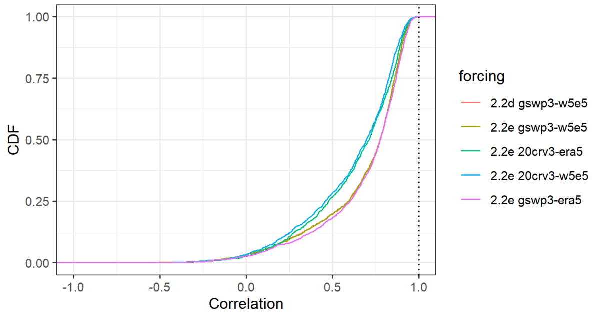

Figure S19. Cumulative distribution of the KGE efficiency metric (correlation parameter) for validation streamflow values at the 1509 gauging stations for all model variants.

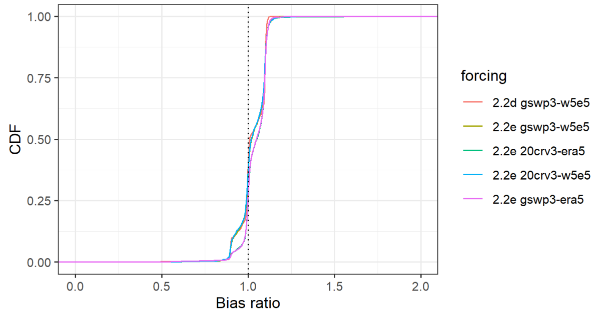

Figure S20. Cumulative distribution of the KGE efficiency metric (bias parameter) for calibration streamflow values at the 1509 gauging stations for all model variants.

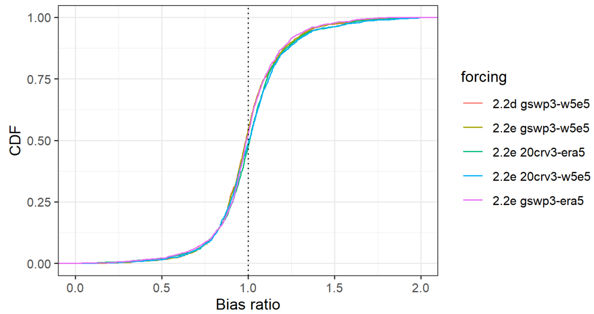

Figure S21. Cumulative distribution of the KGE efficiency metric (bias parameter) for validation streamflow values at the 1509 gauging stations for all model variants.

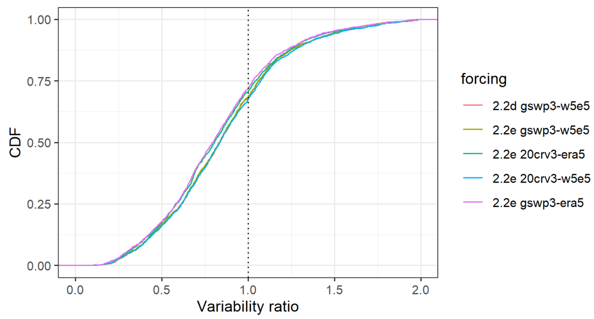

Figure S22. Cumulative distribution of the KGE efficiency metric (variability parameter) for calibration streamflow values at the 1509 gauging stations for all model variants.

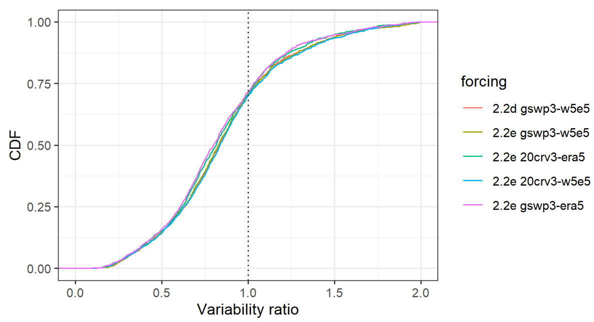

Figure S23. Cumulative distribution of the KGE efficiency metric (variability parameter) for validation streamflow values at the 1509 gauging stations for all model variants.

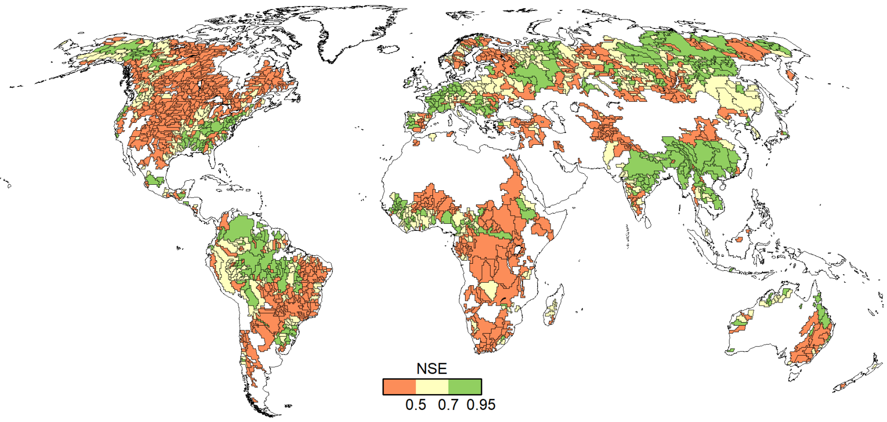

Figure S24. NSE efficiency metric for all monthly data of the 1509 river basins in WaterGAP 2.2d as forced by gswp3-w5e5.

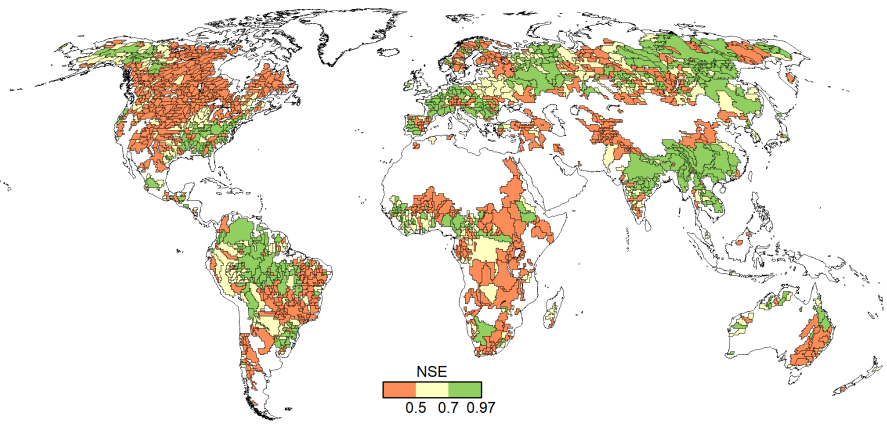

Figure S25. NSE efficiency metric for calibration data of the 1509 river basins in WaterGAP 2.2d as forced by gswp3-w5e5.

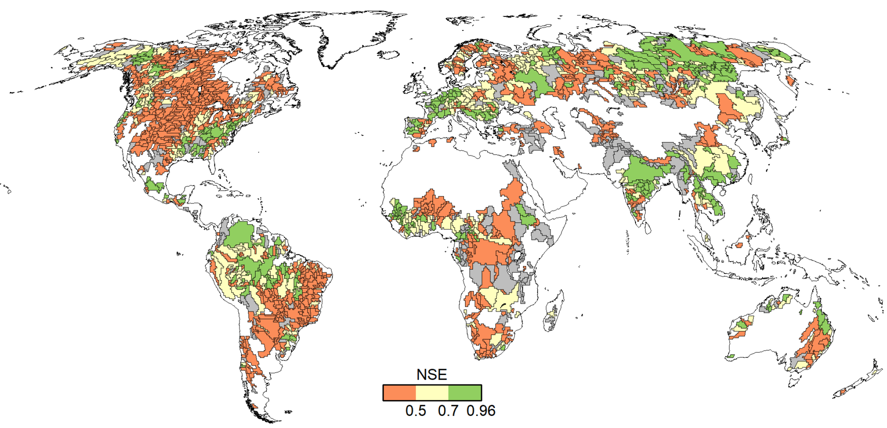

Figure S26. NSE efficiency metric for validation data of the 1509 river basins in WaterGAP 2.2d as forced by gswp3-w5e5. Grey colour indicate that no calculation is possible due to not available observation.

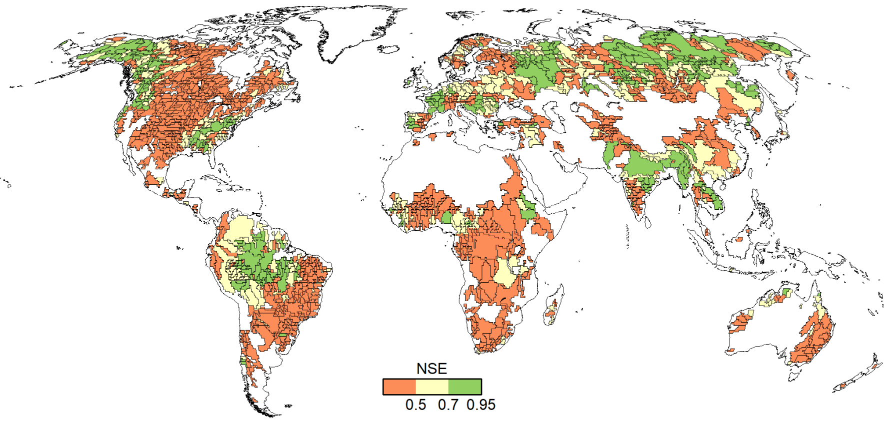

Figure S27. NSE efficiency metric for all monthly data of the 1509 river basins in WaterGAP 2.2e as forced by 20crv3-era5.

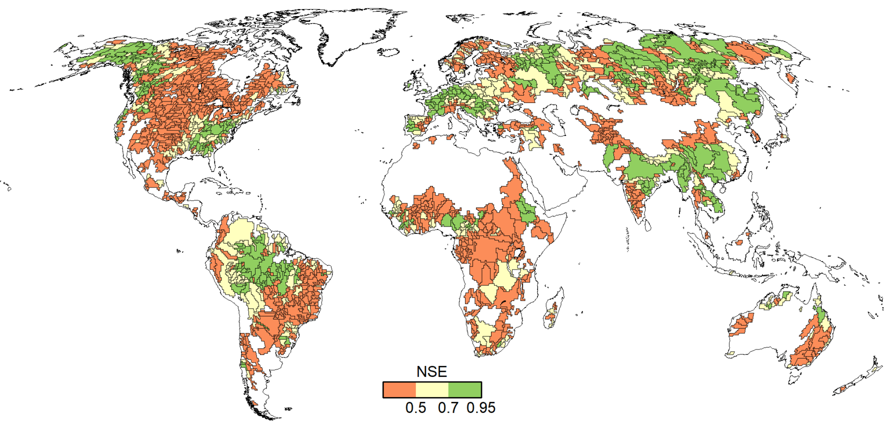

Figure S28. NSE efficiency metric for calibration data of the 1509 river basins in WaterGAP 2.2e as forced by 20crv3-era5.

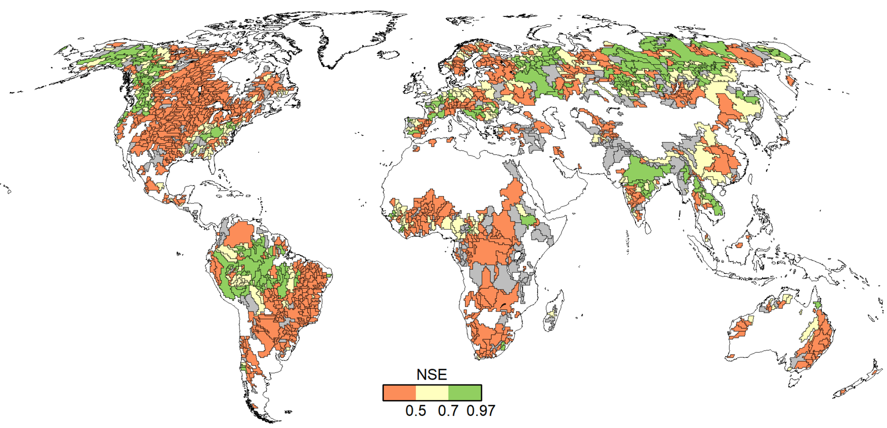

Figure S29. NSE efficiency metric for validation data of the 1509 river basins in WaterGAP 2.2e as forced by 20crv3-era5. Grey colour indicate that no calculation is possible due to not available observation.

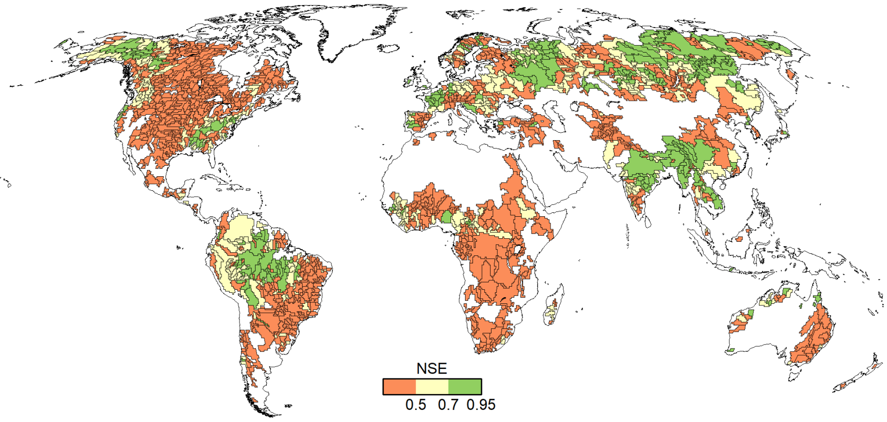

Figure S30. NSE efficiency metric for all monthly data of the 1509 river basins in WaterGAP 2.2e as forced by 20crv3-w5e5.

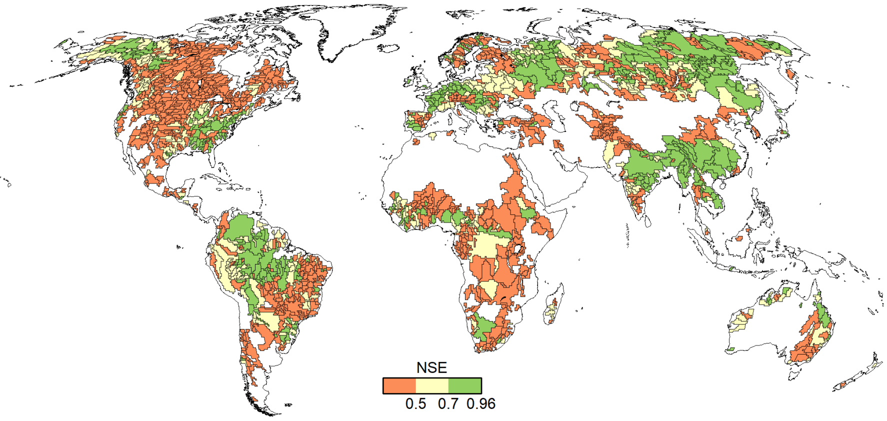

Figure S31. NSE efficiency metric for calibration data of the 1509 river basins in WaterGAP 2.2e as forced by 20crv3-w5e5.

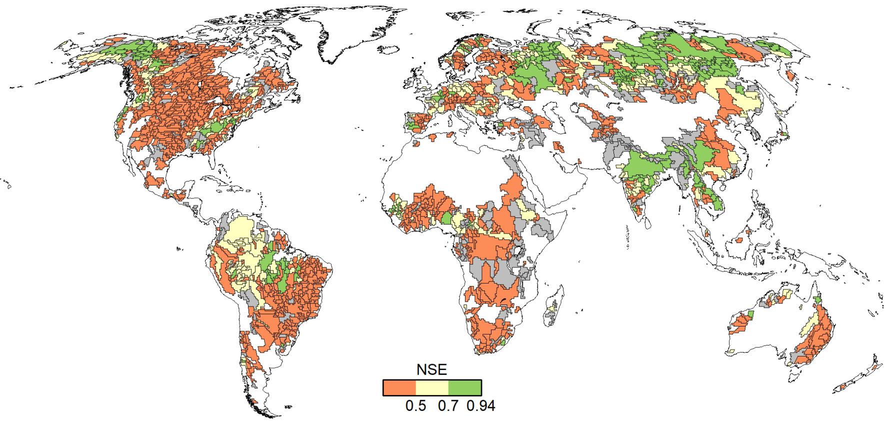

Figure S32. NSE efficiency metric for validation data of the 1509 river basins in WaterGAP 2.2e as forced by 20crv3-w5e5. Grey colour indicate that no calculation is possible due to not available observation.

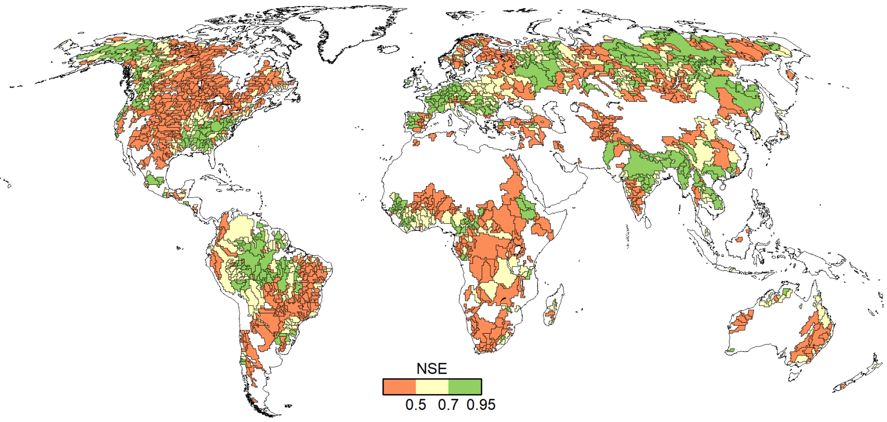

Figure S33. NSE efficiency metric for all monthly data of the 1509 river basins in WaterGAP 2.2e as forced by gswp3-era5.

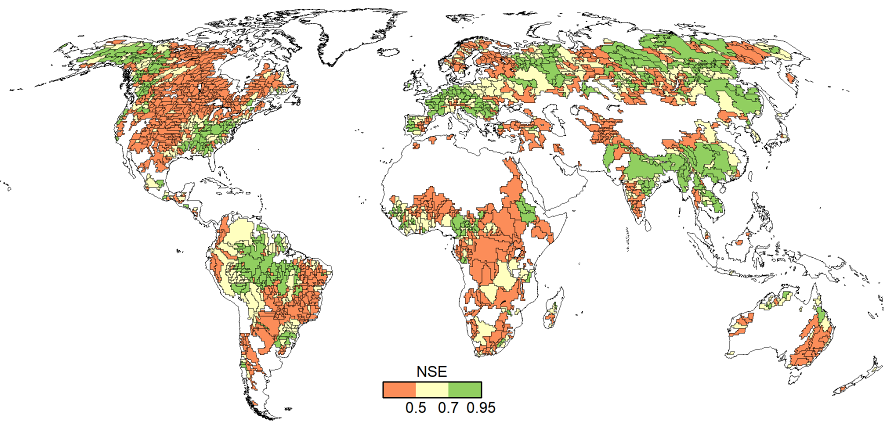

Figure S34. NSE efficiency metric for calibration data of the 1509 river basins in WaterGAP 2.2e as forced by gswp3-era5.

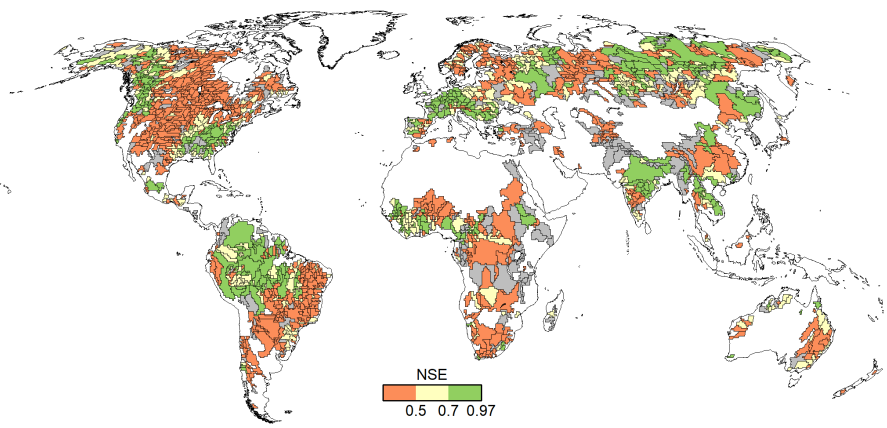

Figure S35. NSE efficiency metric for validation data of the 1509 river basins in WaterGAP 2.2e as forced by gswp3-era5. Grey colour indicate that no calculation is possible due to not available observation.

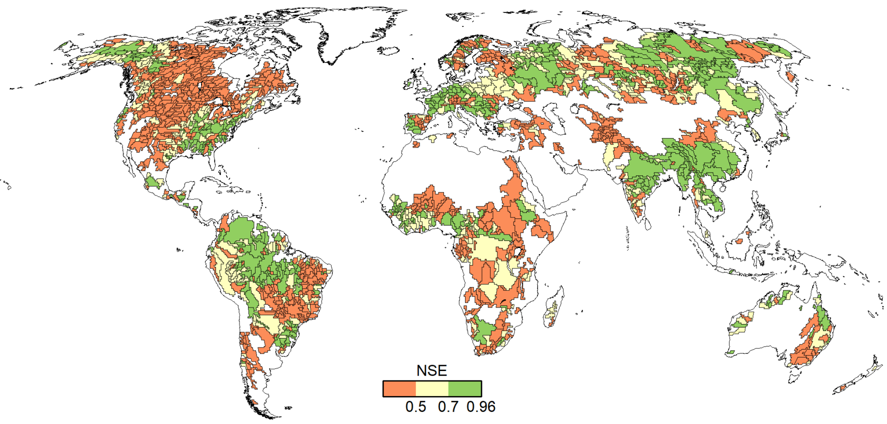

Figure S36. NSE efficiency metric for calibration data of the 1509 river basins in WaterGAP 2.2e as forced by gswp3-w5e5.

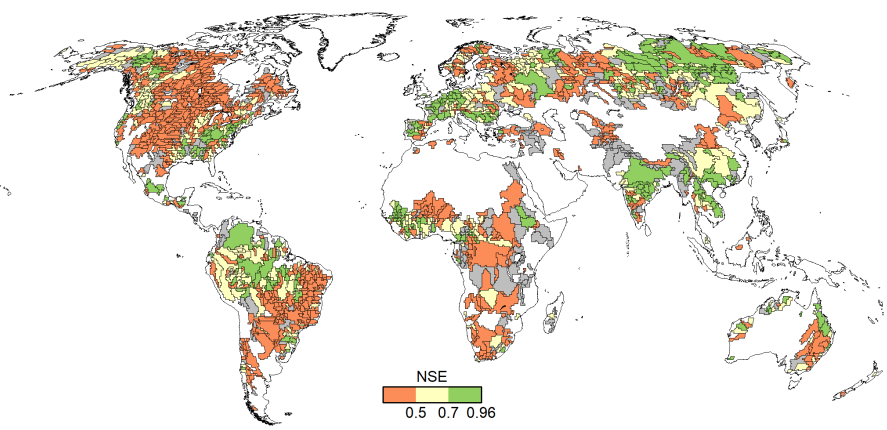

Figure S37. NSE efficiency metric for validation data of the 1509 river basins in WaterGAP 2.2e as forced by gswp3-w5e5. Grey colour indicate that no calculation is possible due to not available observation.

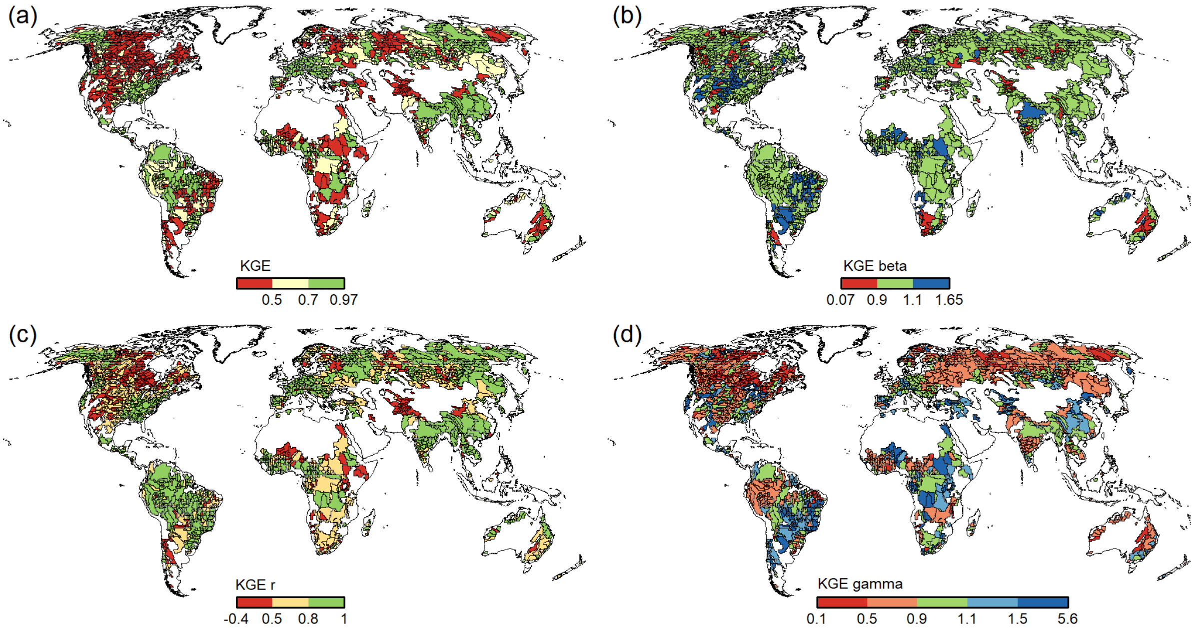

Figure S38. KGE efficiency metric and its components for all monthly streamflow values at the 1509 gauging stations for WaterGAP 2.2d as forced by gswp3-w5e5.

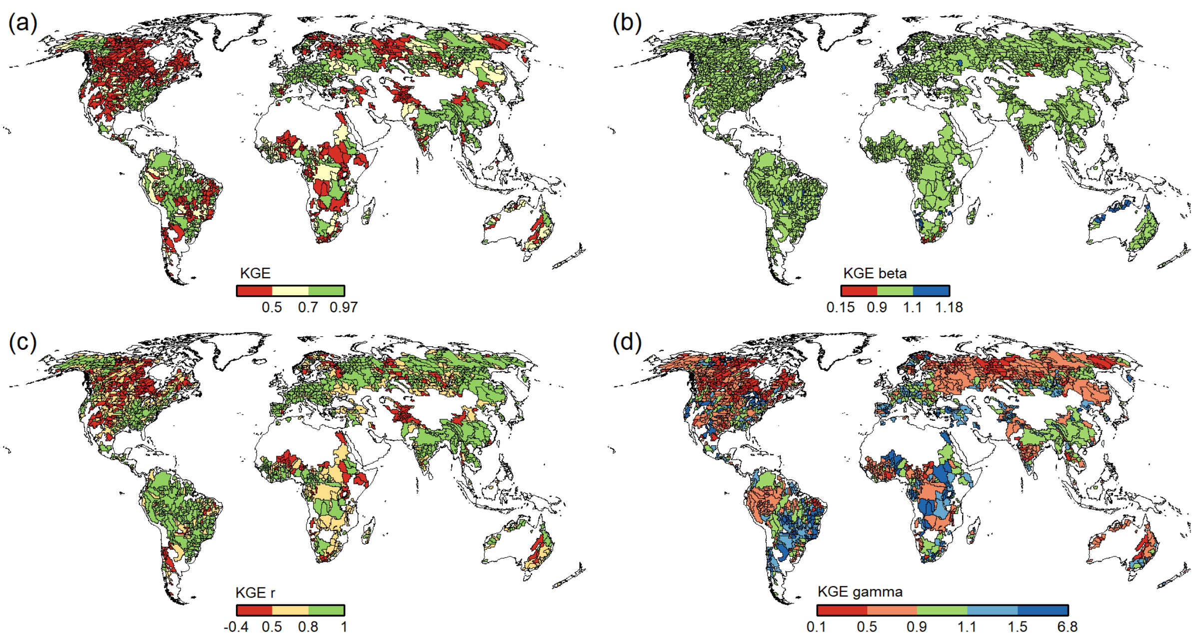

Figure S39. KGE efficiency metric and its components for calibration monthly streamflow values at the 1509 gauging stations for WaterGAP 2.2d as forced by gswp3-w5e5.

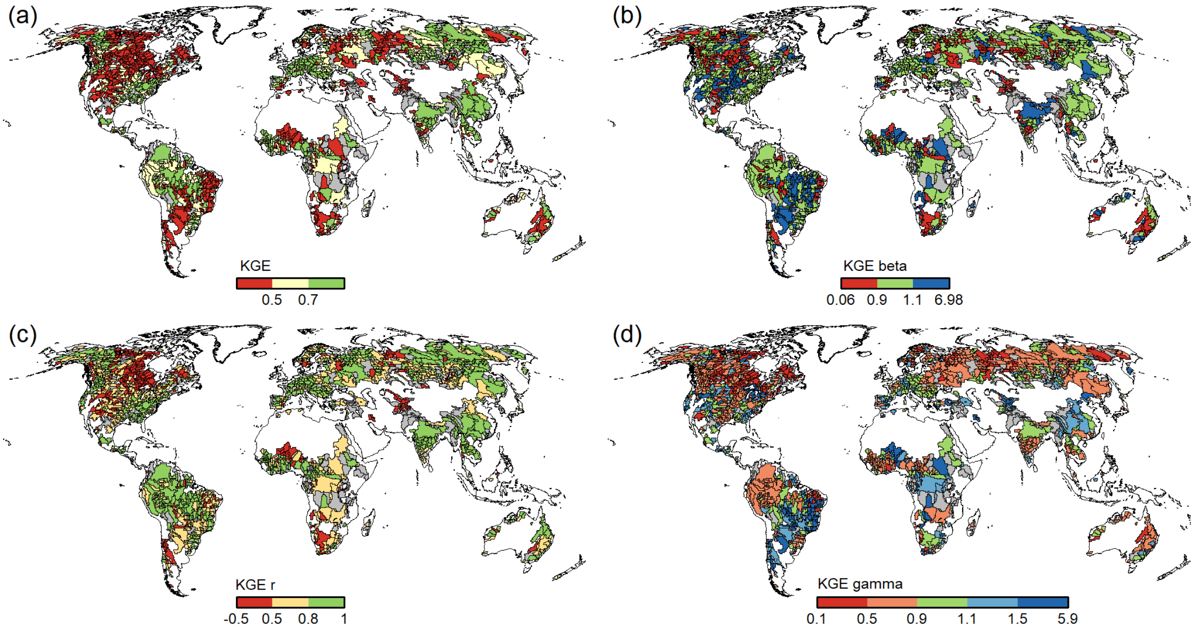

Figure S40. KGE efficiency metric and its components for validation monthly streamflow values at the 1509 gauging stations for WaterGAP 2.2d as forced by gswp3-w5e5. Grey colour indicate that no calculation is possible due to not available observation

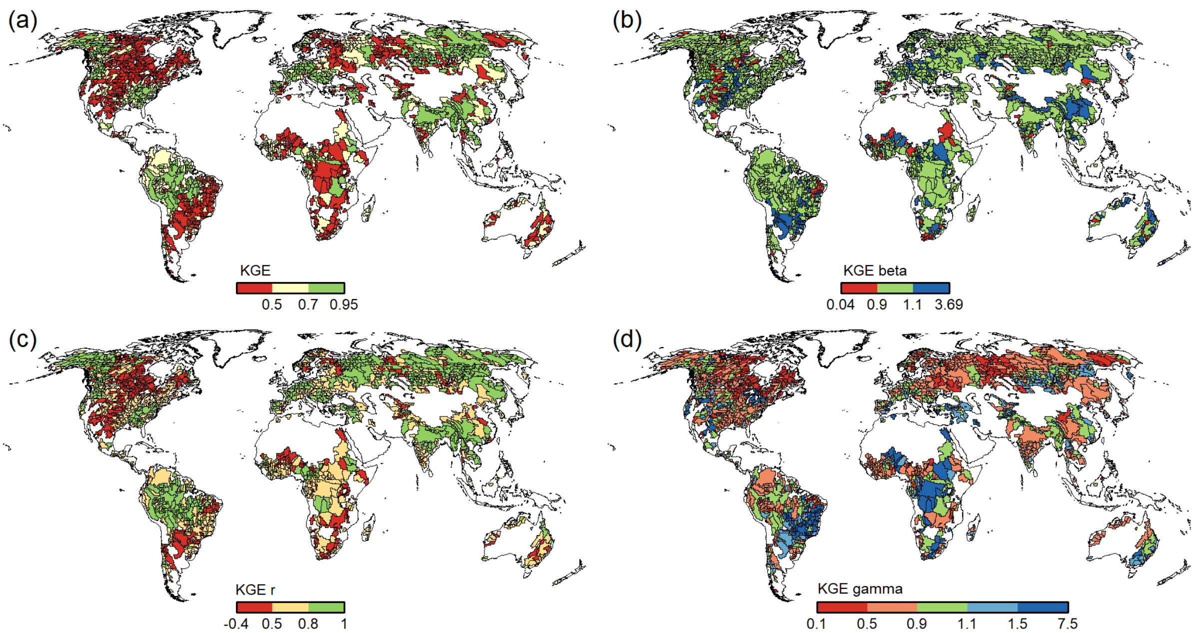

Figure S41. KGE efficiency metric and its components for all monthly streamflow values at the 1509 gauging stations for WaterGAP 2.2e as forced by 20crv3-era5.

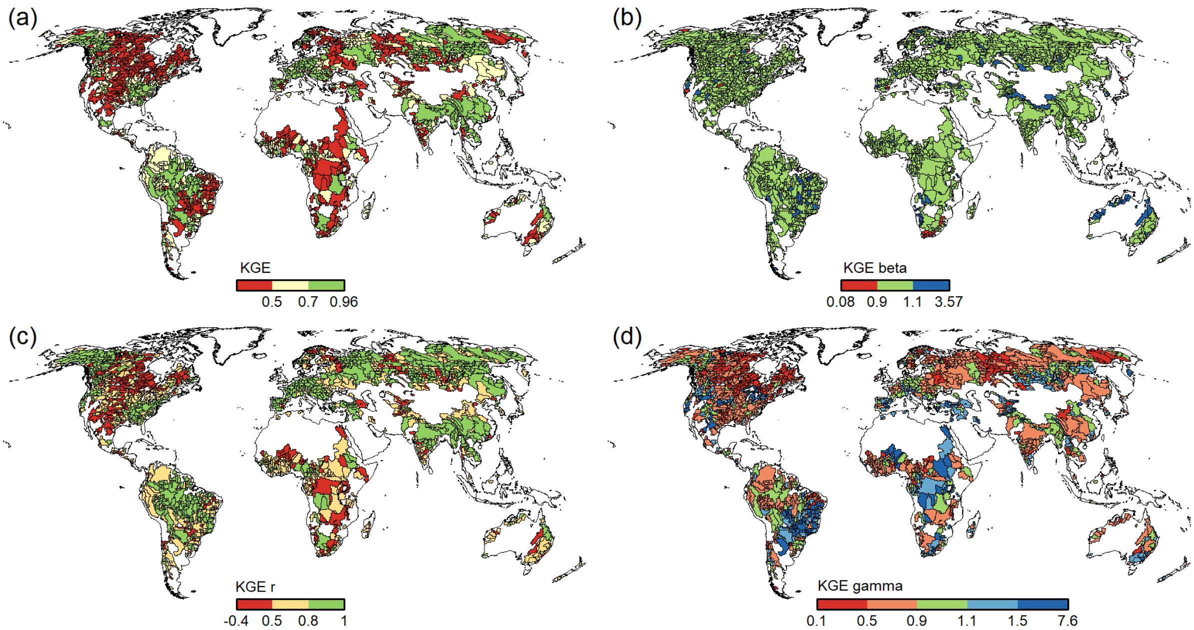

Figure S42. KGE efficiency metric and its components for calibration monthly streamflow values at the 1509 gauging stations for WaterGAP 2.2e as forced by 20crv3-era5.

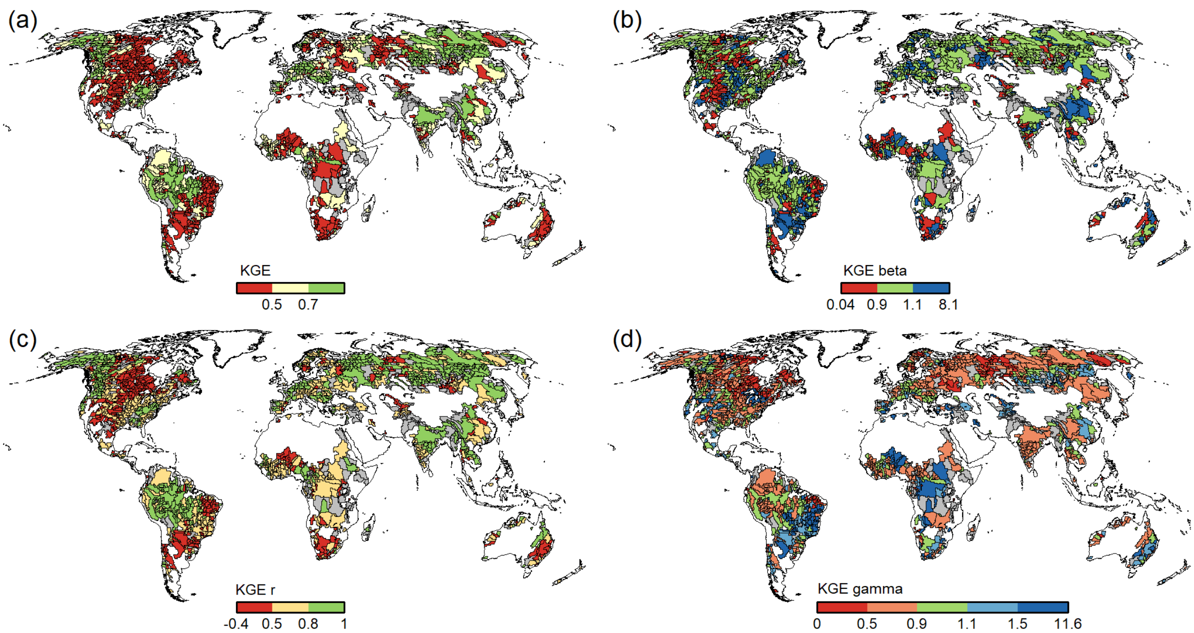

Figure S43. KGE efficiency metric and its components for validation monthly streamflow values at the 1509 gauging stations for WaterGAP 2.2e as forced by 20crv3-era5. Grey colour indicate that no calculation is possible due to not available observation

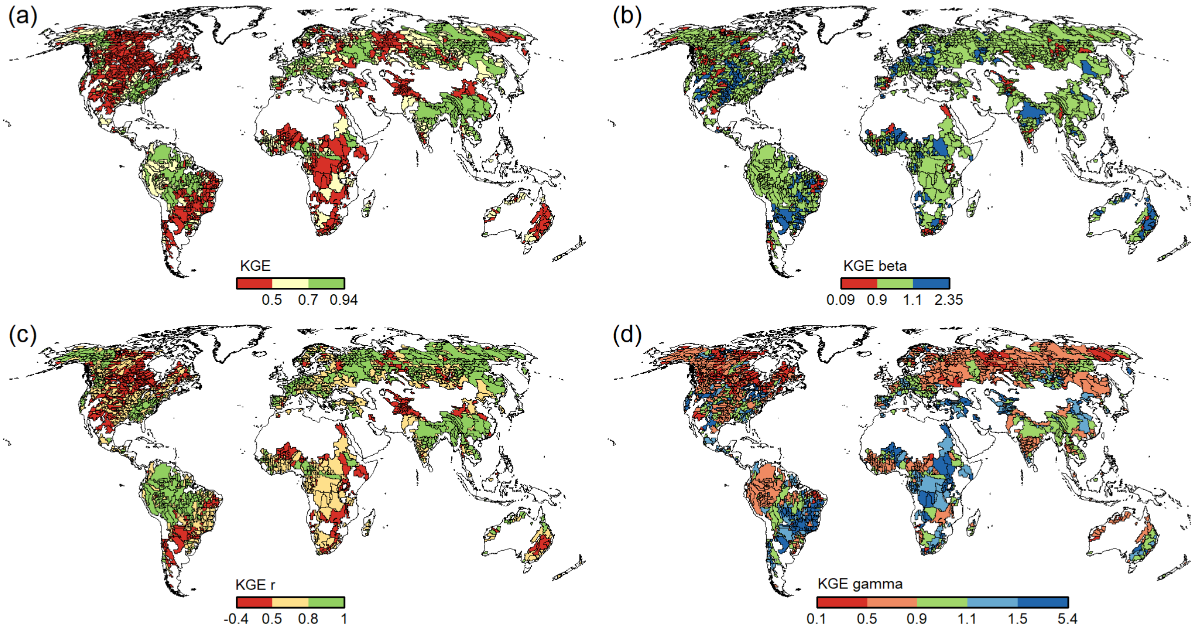

Figure S44. KGE efficiency metric and its components for all monthly streamflow values at the 1509 gauging stations for WaterGAP 2.2e as forced by 20crv3-w5e5.

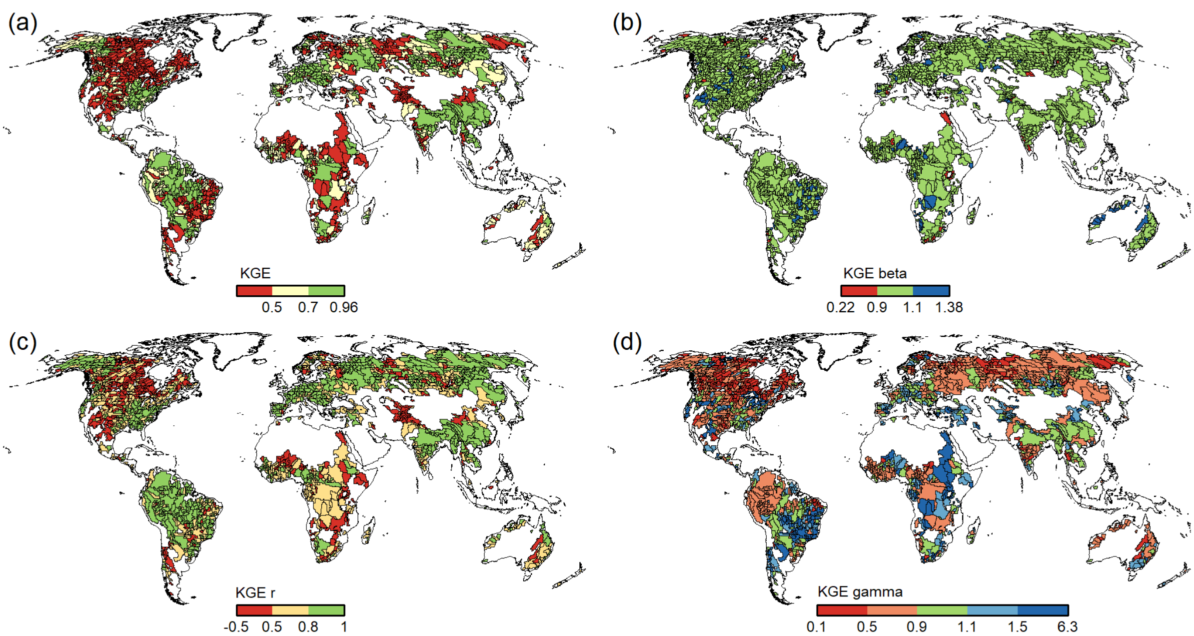

Figure S45. KGE efficiency metric and its components for calibration monthly streamflow values at the 1509 gauging stations for WaterGAP 2.2e as forced by 20crv3-w5e5.

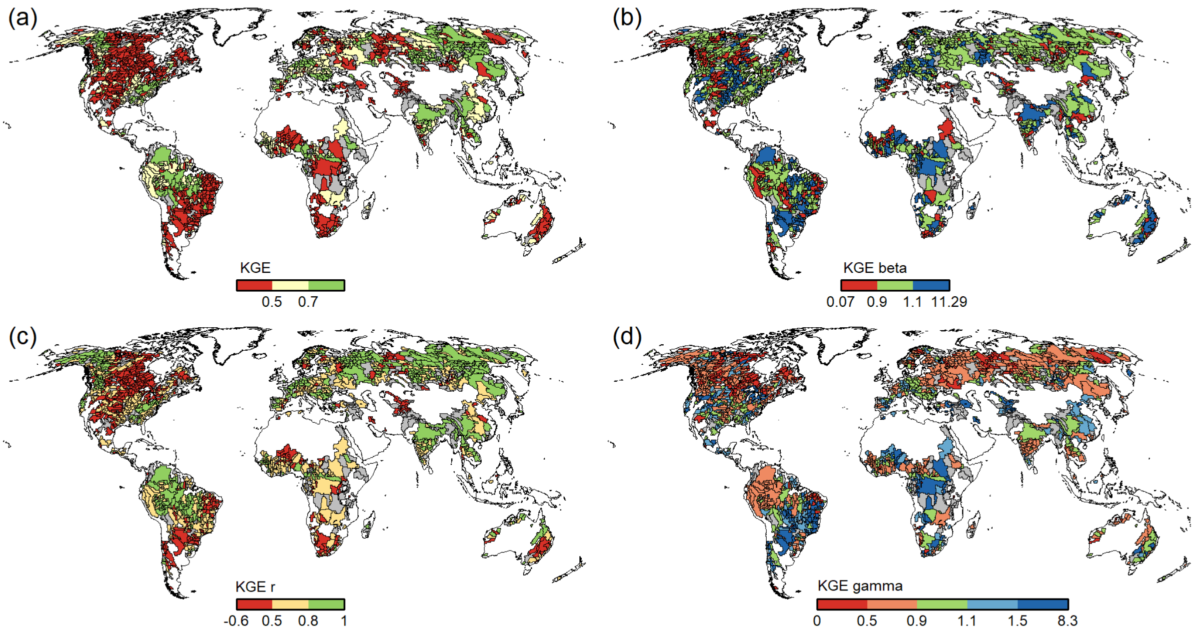

Figure S46. KGE efficiency metric and its components for validation monthly streamflow values at the 1509 gauging stations for WaterGAP 2.2e as forced by 20crv3-w5e5. Grey colour indicate that no calculation is possible due to not available observation

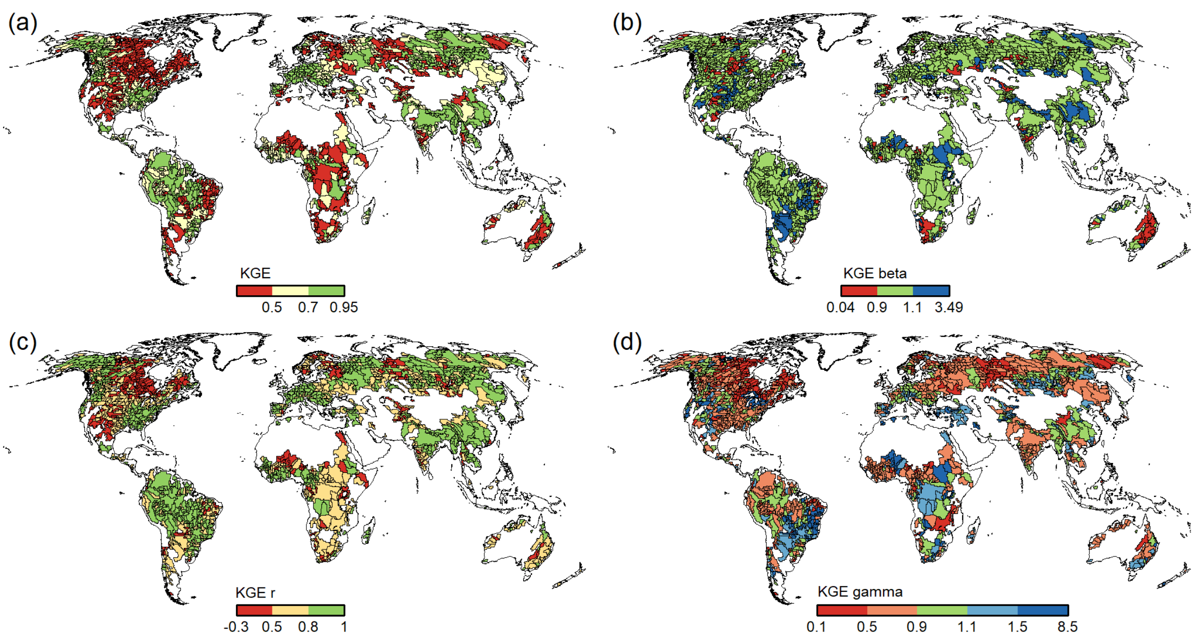

Figure S47. KGE efficiency metric and its components for all monthly streamflow values at the 1509 gauging stations for WaterGAP 2.2e as forced by gswp3-era5.

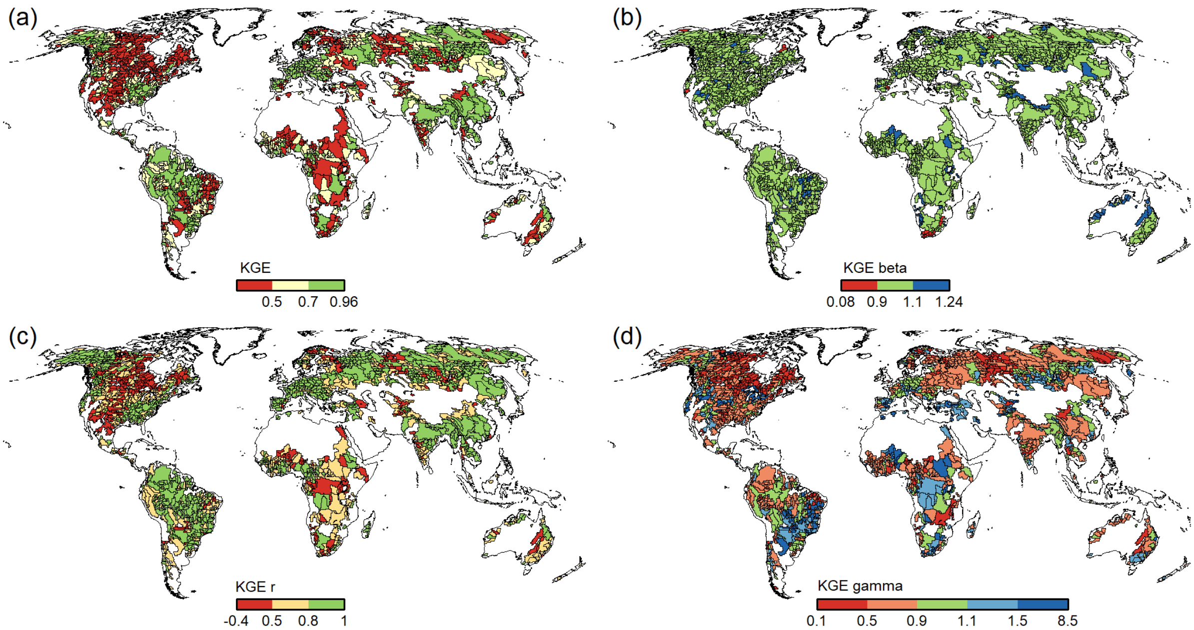

Figure S48. KGE efficiency metric and its components for calibration monthly streamflow values at the 1509 gauging stations for WaterGAP 2.2e as forced by gswp3-era5.

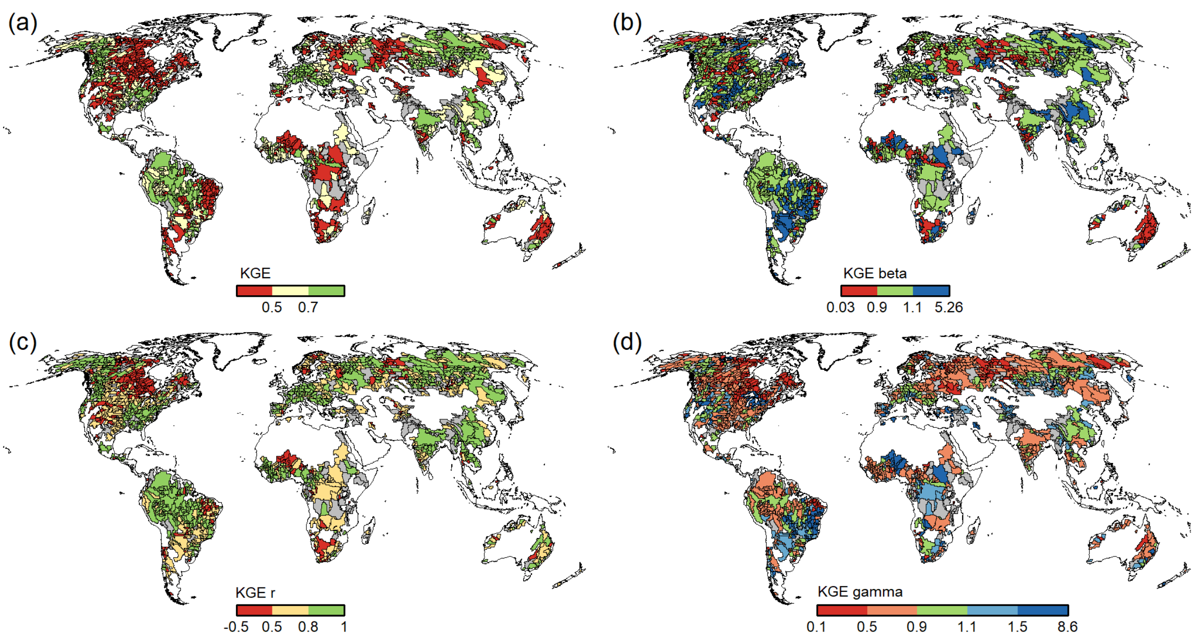

Figure S49. KGE efficiency metric and its components for validation monthly streamflow values at the 1509 gauging stations for WaterGAP 2.2e as forced by gswp3-era5. Grey colour indicate that no calculation is possible due to not available observation

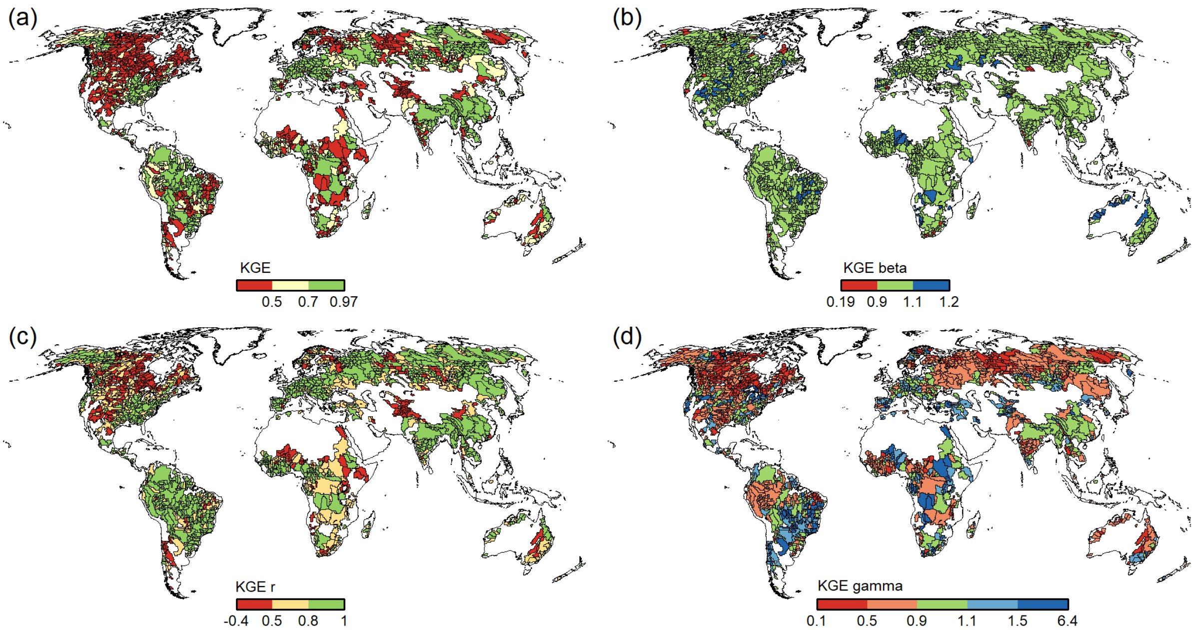

Figure S50. KGE efficiency metric and its components for calibration monthly streamflow values at the 1509 gauging stations for WaterGAP 2.2e as forced by gswp3-w5e5.

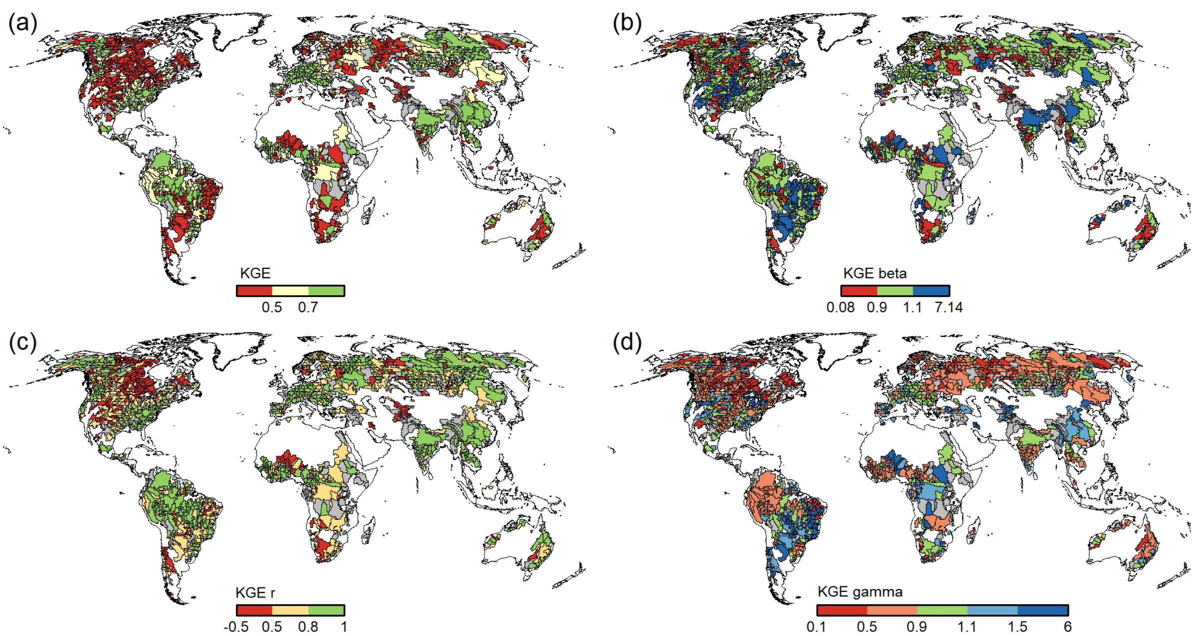

Figure S51. KGE efficiency metric and its components for validation monthly streamflow values at the 1509 gauging stations for WaterGAP 2.2e as forced by gswp3-w5e5. Grey colour indicate that no calculation is possible due to not available observation

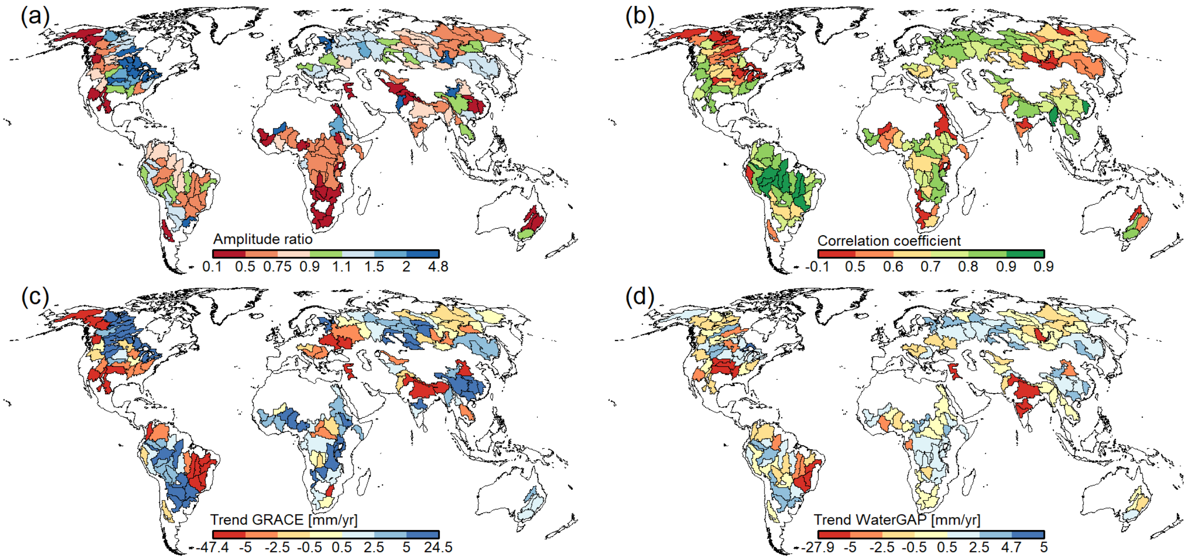

Figure S52. Comparison of basin-average TWSAs of WaterGAP 2.2d as forced by gswp3-w5e5 and GRACE for 148 basins larger than 200000 km^2, with (a) ratio of amplitude (reddish colors indicate underestimated amplitude of WaterGAP, vice versa for bluish), (b) correlation coefficient, (c) trend of GRACE and (d) trend of WaterGAP 2.2d. All values based on the time series January 2003 - December 2019.

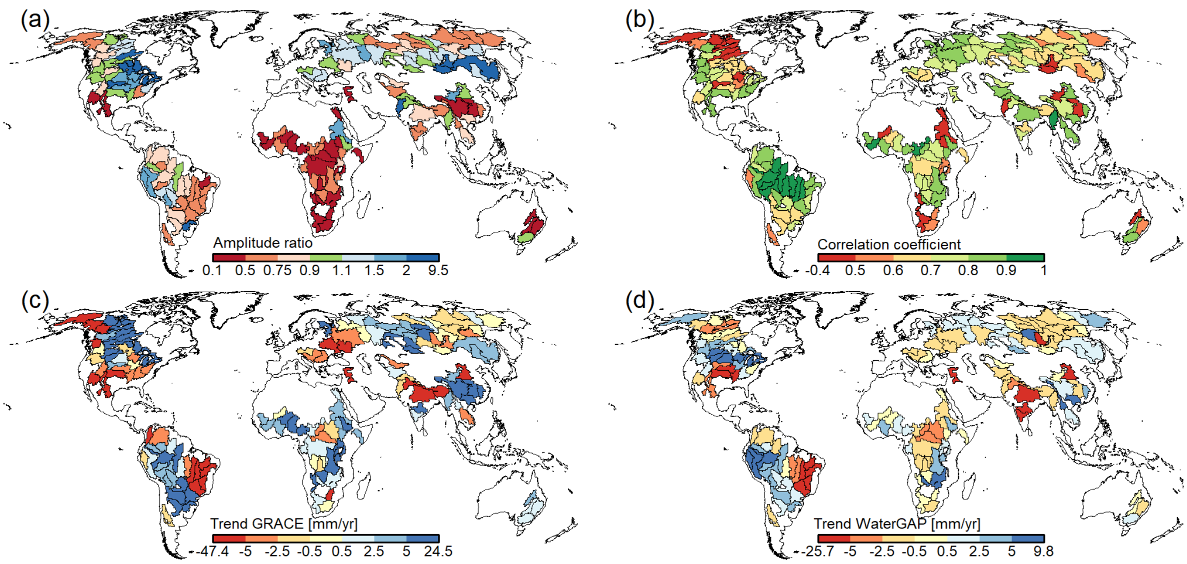

Figure S53. Comparison of basin-average TWSAs of WaterGAP 2.2e as forced by gswp3-era5 and GRACE for 148 basins larger than 200000 km^2, with (a) ratio of amplitude (reddish colors indicate underestimated amplitude of WaterGAP, vice versa for bluish), (b) correlation coefficient, (c) trend of GRACE and (d) trend of WaterGAP 2.2e. All values based on the time series January 2003 - December 2019.

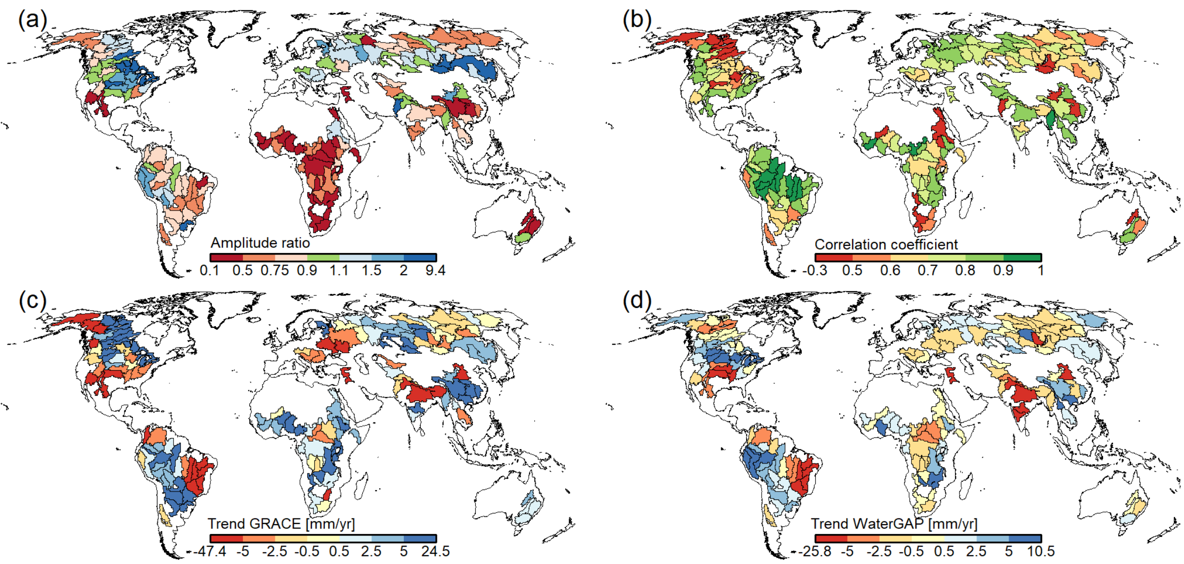

Figure S54. Comparison of basin-average TWSAs of WaterGAP 2.2e as forced by 20crv3-era5 and GRACE for 148 basins larger than 200000 km^2, with (a) ratio of amplitude (reddish colors indicate underestimated amplitude of WaterGAP, vice versa for bluish), (b) correlation coefficient, (c) trend of GRACE and (d) trend of WaterGAP 2.2e. All values based on the time series January 2003 - December 2019.

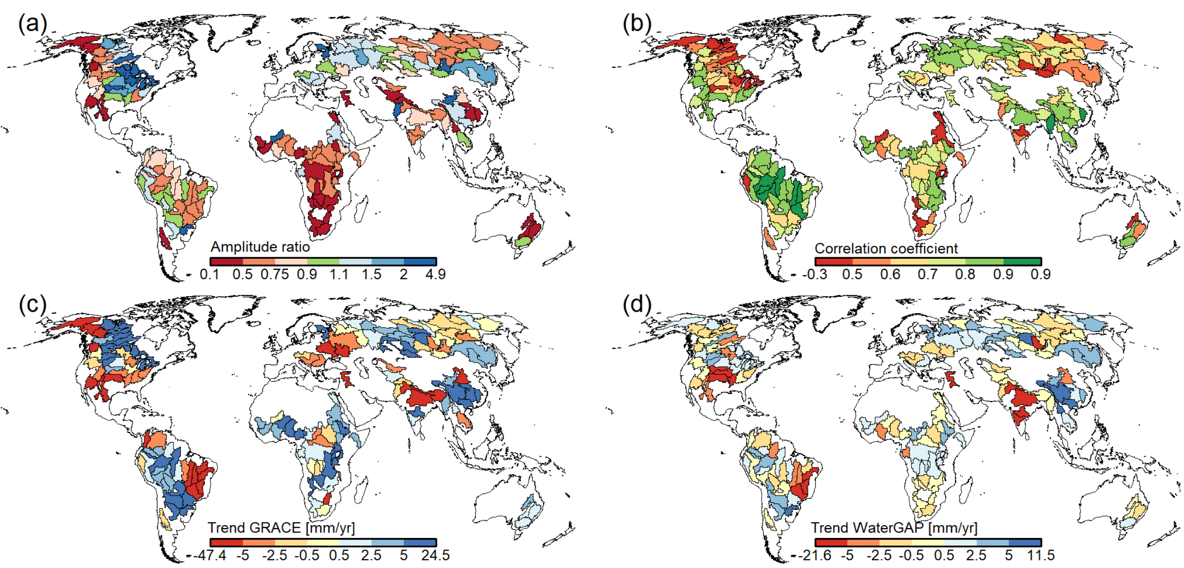

Figure S55. Comparison of basin-average TWSAs of WaterGAP 2.2e as forced by 20crv3-w5e5 and GRACE for 148 basins larger than 200000 km^2, with (a) ratio of amplitude (reddish colors indicate underestimated amplitude of WaterGAP, vice versa for bluish), (b) correlation coefficient, (c) trend of GRACE and (d) trend of WaterGAP 2.2e. All values based on the time series January 2003 - December 2019.

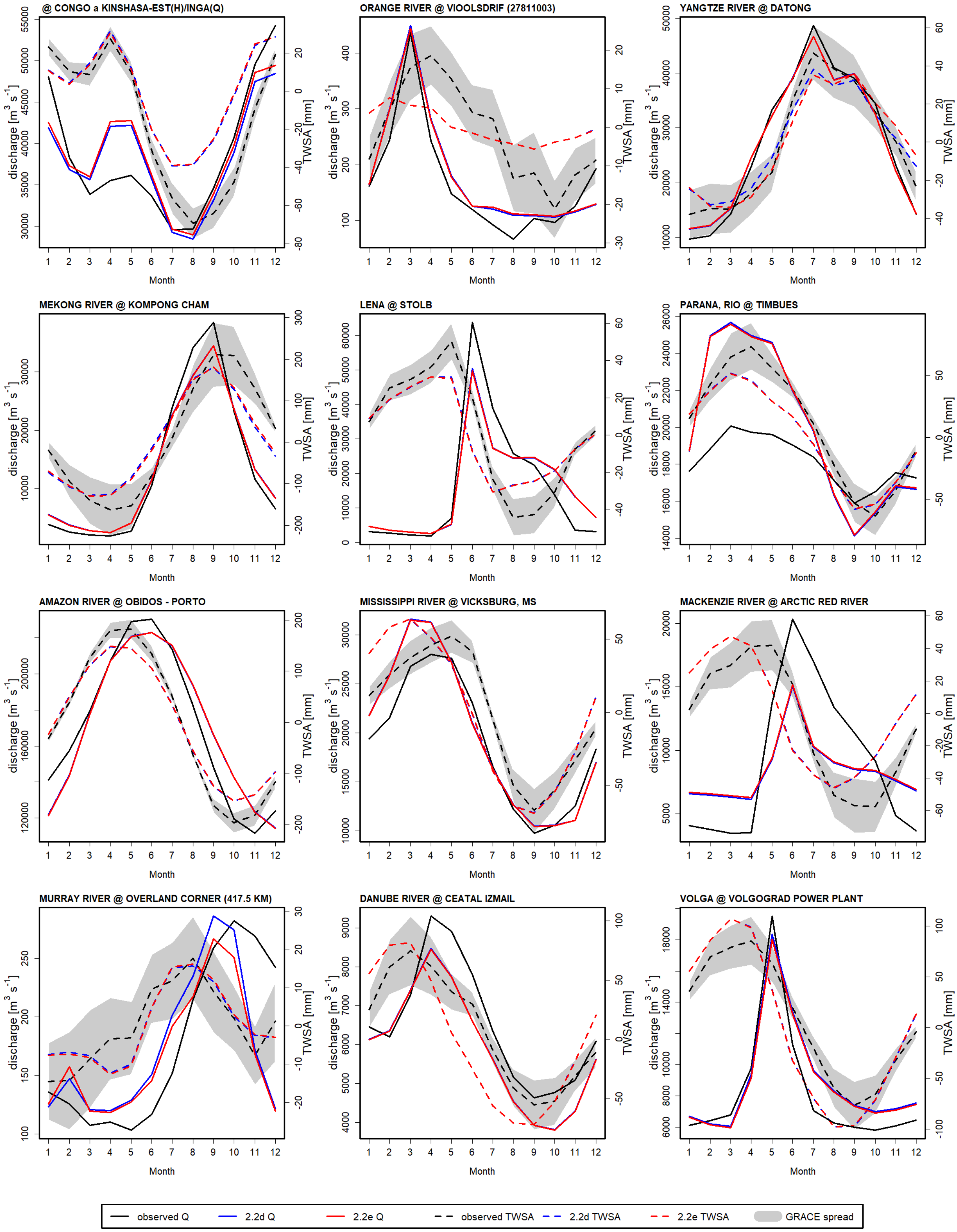

Figure S56. Seasonality of streamflow and TWSAs of selected large river basins: model results of WaterGAP 2.2e and WaterGAP 2.2d with gswp3-w5e5 as forcing as well as streamflow and TWSA observations.

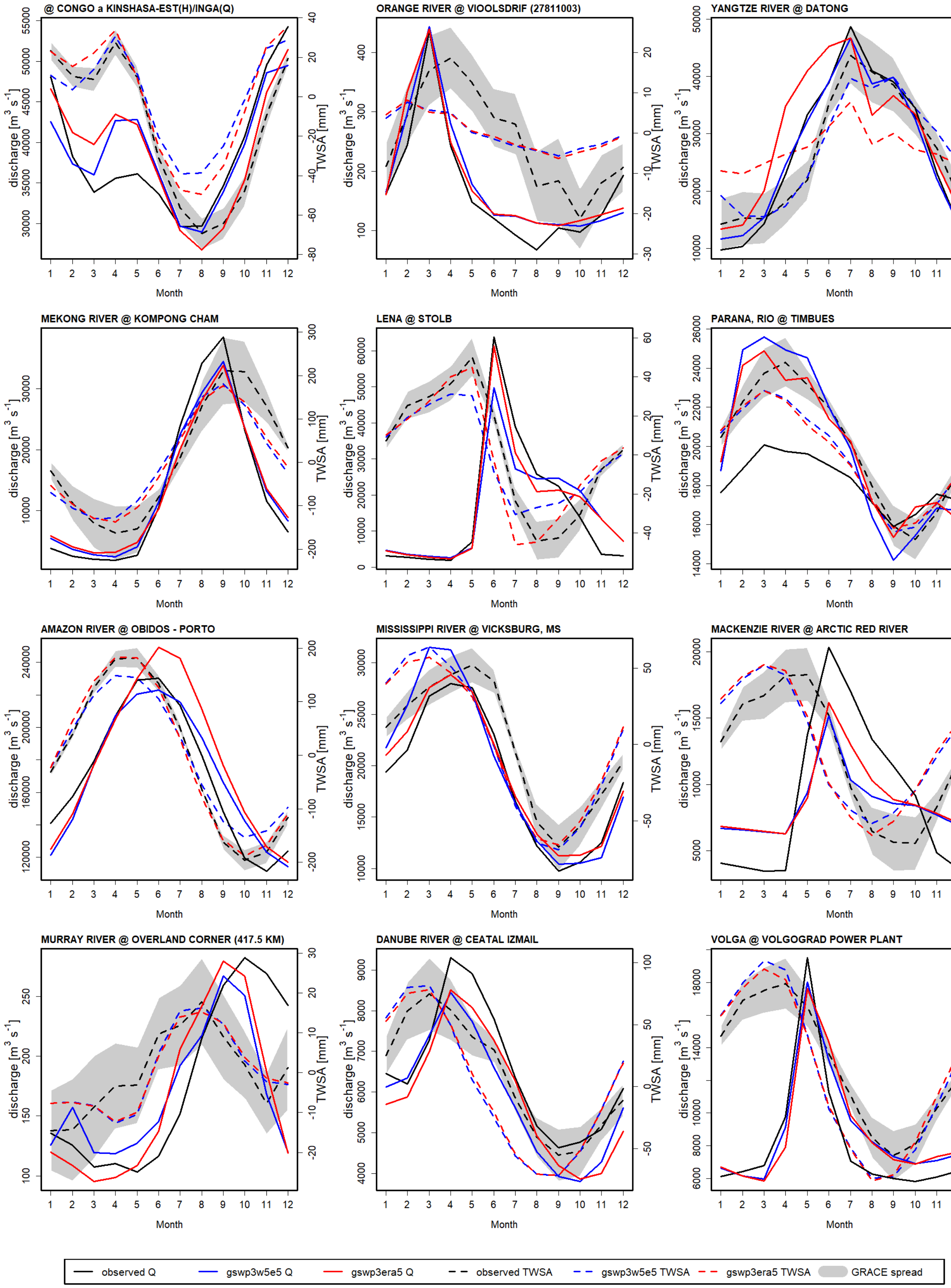

Figure S57. Seasonality of streamflow and TWSAs of selected large river basins: model results of WaterGAP 2.2e with gswp3-w5e5 and gswp3-era5 as forcing as well as streamflow and TWSA observations.

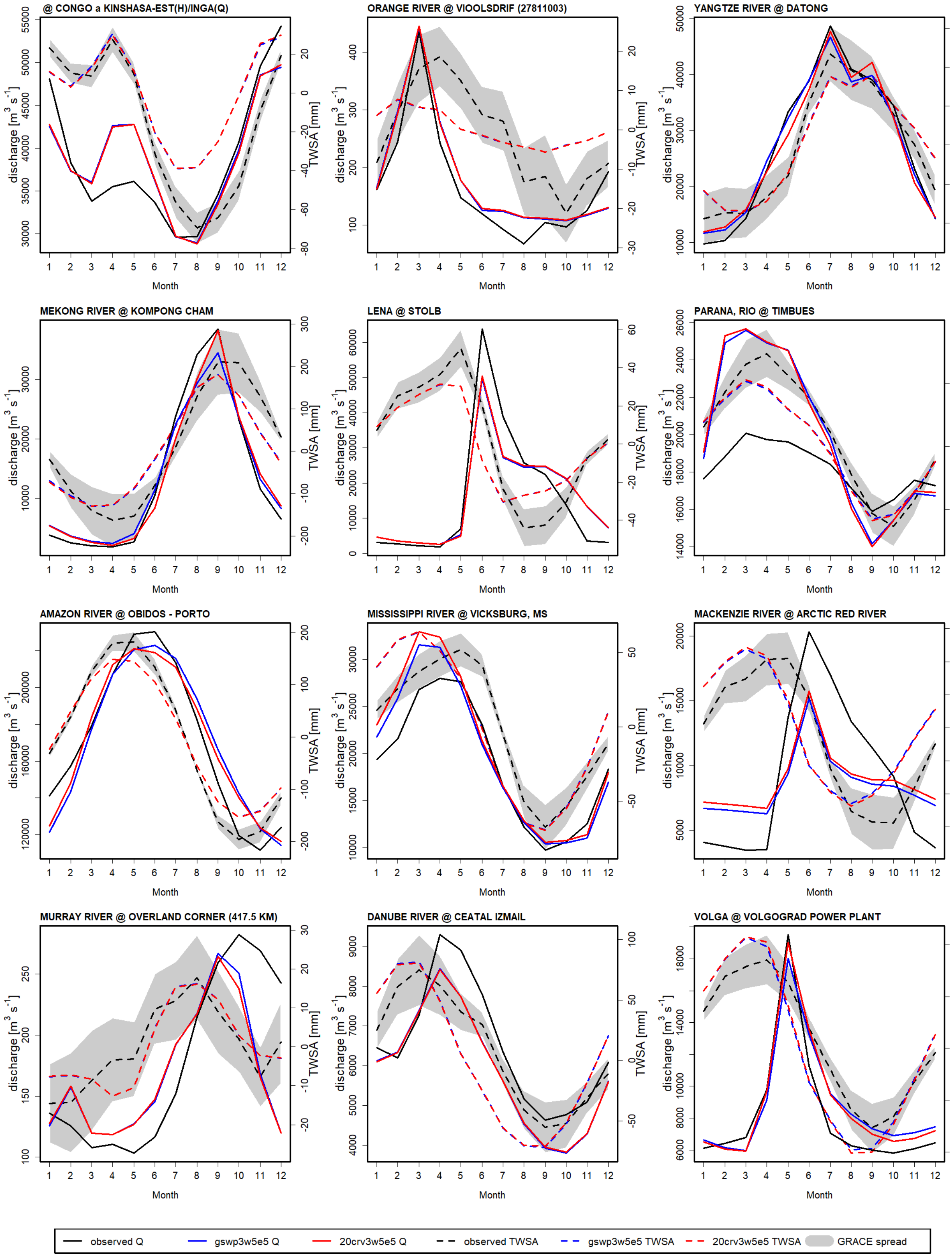

Figure S58. Seasonality of streamflow and TWSAs of selected large river basins: model results of WaterGAP 2.2e with gswp3-w5e5 and 20crv3-w5e5 as forcing as well as streamflow and TWSA observations.

References

Bureau of Reclamation: Hydromet Historical Data Access, https://www.usbr.gov/pn/hydromet/arcread.html.

California Department of Water Resources: California Data Exchange Center, https://cdec.water.ca.gov/misc/resinfo.html.

FAO: AQUASTAT, https://www.fao.org/aquastat/en/databases/maindatabase, 2023.

Müller Schmied, H., Cáceres, D., Eisner, S., Flörke, M., Herbert, C., Niemann, C., Peiris, T. A., Popat, E., Portmann, F. T., Reinecke, R., Schumacher, M., Shadkam, S., Telteu, C.-E., Trautmann, T., and Döll, P.: The global water resources and use model WaterGAP v2.2d: model description and evaluation, Geoscientific Model Development, 14, 1037–1079, https://doi.org/10.5194/gmd-14-1037-2021, https://gmd.copernicus.org/articles/14/1037/2021/, 2021.

Texas Water Development Board: Water Data for Texas, https://waterdatafortexas.org/reservoirs/statewide.